Combined Analysis

texture, structure, microstructure, phase, stresses and reflectivity investigations of real multi-phased ceramics and thin structures using scattering of rays

Daniel Chateigner
CRISMAT-ENSICAEN (Caen-France)

Bi2223 Superconductors

PCT Ferroelectrics

Irradiated FAp ceramics

$Ca_3Co_4O_9$ Thermoelectrics

nano-Si thin films

AlN/Pt/Ni(Co) thick films

Texture from Spectra

Orientation Distribution Function (ODF)

From pole figures

From spectra

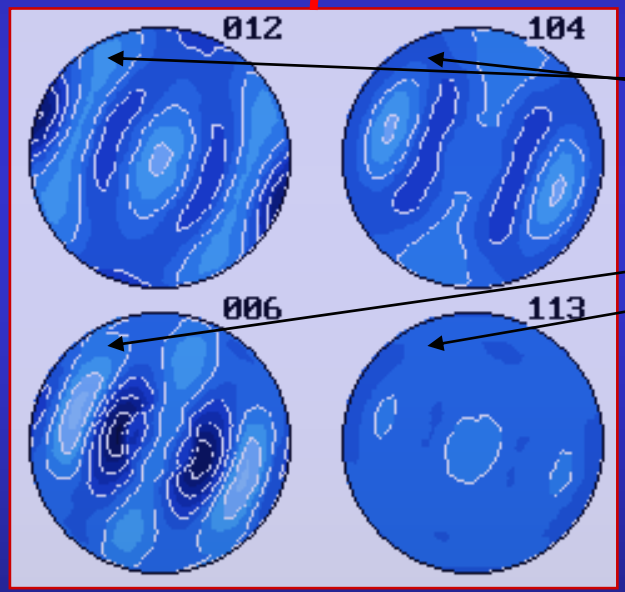

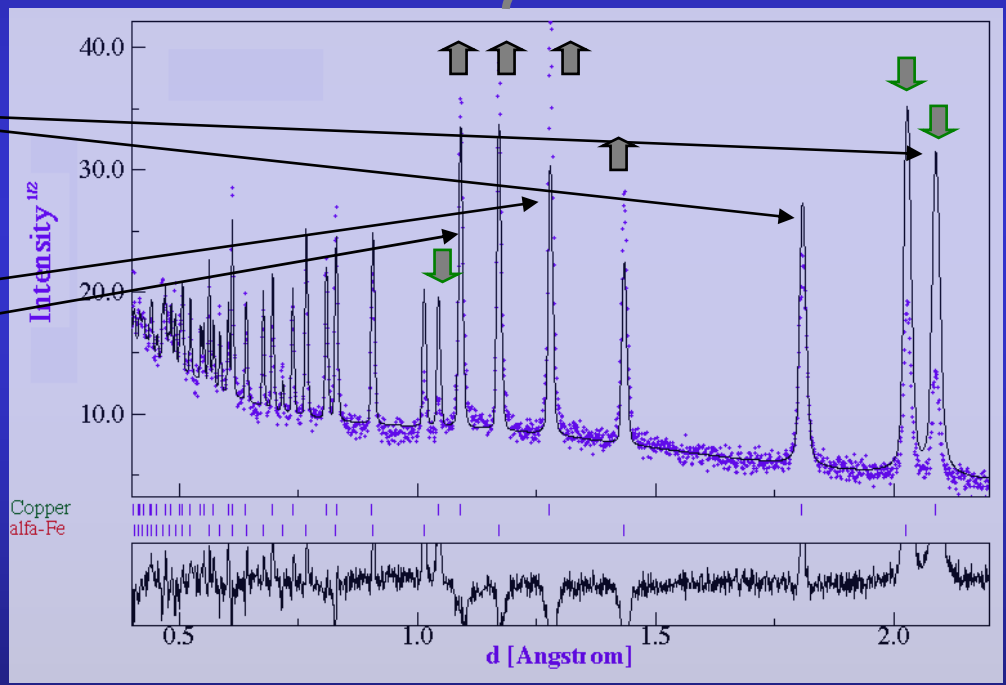

Residual Stresses and Rietveld

- Macro elastic strain tensor (I kind)
- Crystal anisotropic strains (II kind)

C

Macro and micro stresses

Applied macro stresses

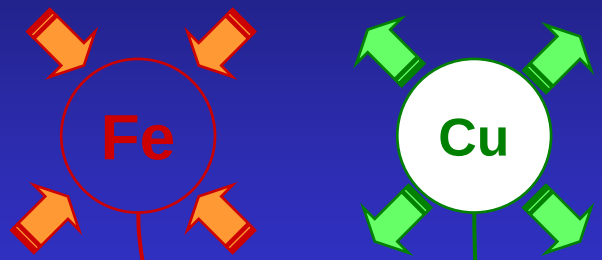

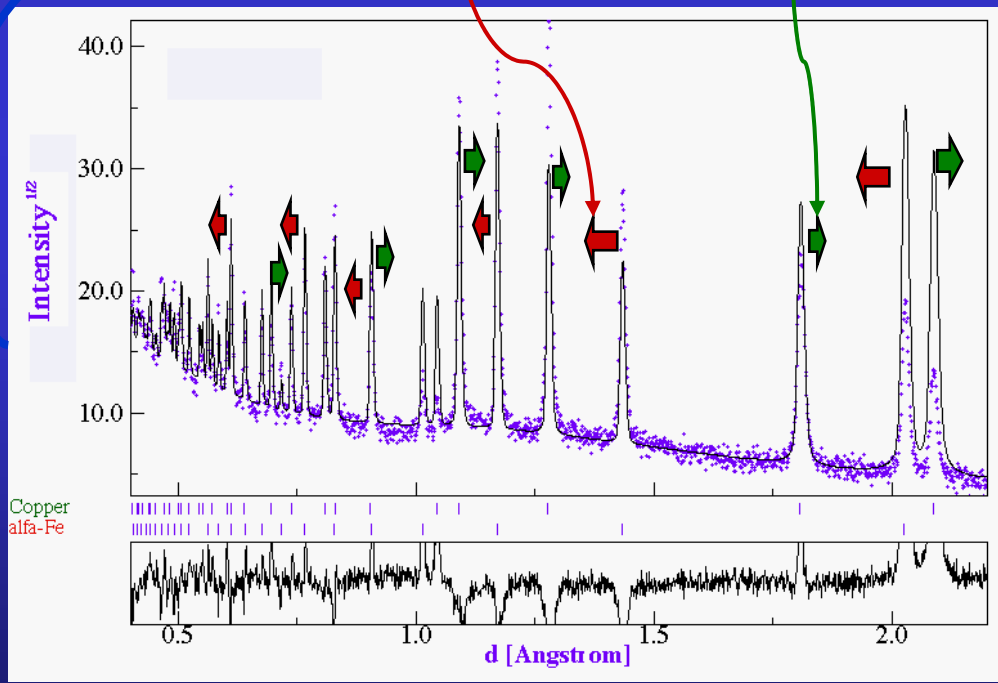

Textured samples: Reuss, Voigt, Hill, Bulk geometric mean approaches

How it works

Le Bail extraction

$$T_{hkl}^{k} = T_{hkl}^{k-1} \frac{\sum_i I_i^{\exp} S_{hkl}^{i}}{\sum_i I_i^{calc} S_{hkl}^{i}}$$

- Starts with nominal intensities (T_{hkl})
- Computes the full pattern (I^{calc})
- Uses the formula to compute next T_{hkl}
- Cycle the last two steps until convergence

- In Maud, options:
  - Only few cycles for texture (3-5) necessary
  - The range for the weighting of the profile can be reduced
  - Background subtracted or not

Minimization algorithms

- Can be fully used in the method (everywhere)

- Marquardt Least Squares (based on steepest decrease and Gauss-Newton)
  - Efficient, best with few parameters, near the solution
- Evolutionary computation (or genetic algorithm)
  - Slow, not efficient, requires a lot of resources
  - Unlimited number of parameters
  - Can start far from the solution
- Simulated annealing (the solution proceed like a random walk, but the walking step decreases as temperature decreases)
  - In between the Marquardt and evolutionary algorithms
- Simplex (generates n+1 starting solutions as vertices of a polygon, n number of parameters, and contract/expand the polygon around the minima)
  - Slow on convergence
  - Remains close to the solution, but explore more minima with respect to the Marquardt

Anisotropic sizes and microstrains

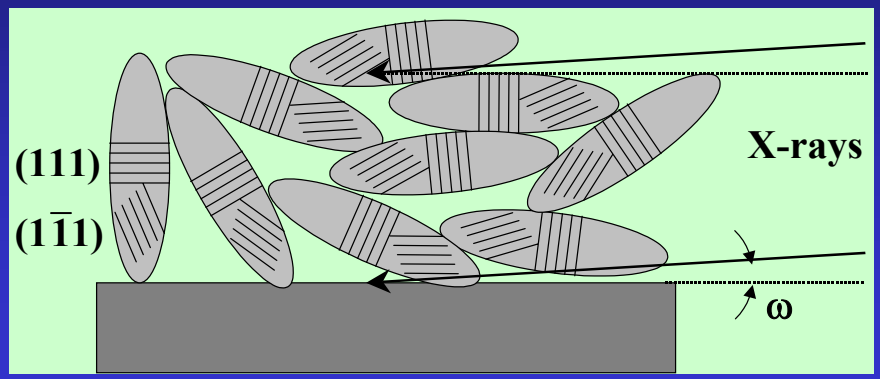

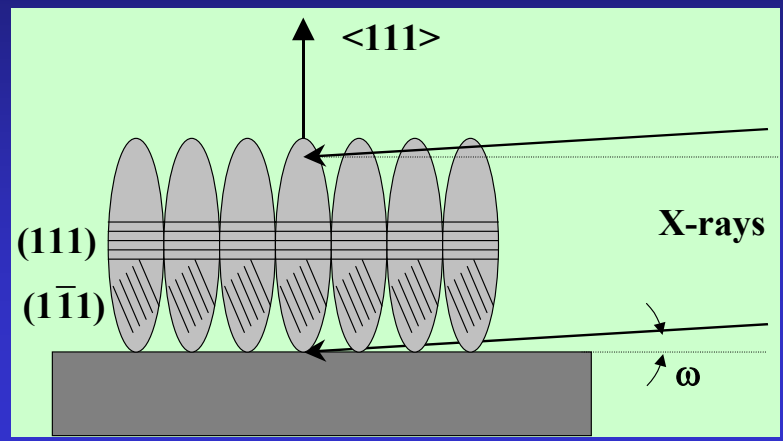

- Texture helps the "real" mean shape determination
- Determination by peak deconvolution + Popa formalism

$$\langle R_{\mathbf{h}} \rangle = R_0 + R_1 P_2^{\,0}(x) + R_2 P_2^{\,1}(x)\cos\varphi + R_3 P_2^{\,1}(x)\sin\varphi + R_4 P_2^{\,2}(x)\cos 2\varphi + R_5 P_2^{\,2}(x)\sin 2\varphi + \ldots$$

$$\langle \varepsilon_{\mathbf{h}}^{\,2} \rangle E_{\mathbf{h}}^{\,4} = E_1 h^4 + E_2 k^4 + E_3 \ell^4 + 2E_4 h^2 k^2 + 2E_5 \ell^2 k^2 + 2E_6 h^2 \ell^2 + 4E_7 h^3 k + 4E_8 h^3 \ell + 4E_9 k^3 h + 4E_{10} k^3 \ell + 4E_{11} \ell^3 h + 4E_{12} \ell^3 k + 4E_{13} h^2 k \ell + 4E_{14} k^2 h \ell + 4E_{15} \ell^2 k h$$

Rietveld-Structure

$$I_i^{calc}(\chi,\phi) = \sum_{n=1}^{Nphases} S_n \sum_k L_k \left|F_{k;n}\right|^2 S(2\theta_i - 2\theta_{k;n}) P_{k;n}(\chi,\phi) A + bkg_i$$

Texture

$$P_k(\chi,\phi) = \int_{\varphi} f(g,\varphi) d\varphi$$

- Generalized Spherical Harmonics (Bunge):

$$P_k(\chi,\phi) = \sum_{l=0}^{\infty} \frac{1}{2l+1} \sum_{n=-l}^{l} k_l^n(\chi,\phi) \sum_{m=-l}^{l} C_l^{mn} k_n^{*m}(\Theta_k \phi_k)$$

$$f(g) = \sum_{l=0}^{\infty} \sum_{m,n=-l}^{l} C_l^{mn} T_l^{mn}(g)$$

- Components (Helming):

$$f(g) = F + \sum_c I^c f^c(g)$$

- WIMV (William, Imhof, Matthies, Vinel) iterative process:

$$f^{n+1}(g) = N_n \frac{f^n(g) f^0(g)}{\left(\prod_{\mathbf{h}=1}^{\mathrm{I}} \prod_{m=1}^{M_\mathbf{h}} P_\mathbf{h}^n(\mathbf{y}) \right)^{\frac{1}{IM_\mathbf{h}}}}$$

$$f^0(g) = N_0 \left(\prod_{\mathbf{h}=1}^{\mathrm{I}} \prod_{m=1}^{M_\mathbf{h}} P_\mathbf{h}^{\exp}(\mathbf{y}) \right)^{\frac{1}{IM_\mathbf{h}}}$$

E-WIMV (Rietveld only):

with $0 < r_n < 1$, relaxation parameter,
$M_\mathbf{h}$ number of division points of the integral around k,
$w_\mathbf{h}$ reflection weight

$$f^{n+1}(g) = f^n(g) \prod_{m=1}^{M_\mathbf{h}} \left(\frac{P_\mathbf{h}(\mathbf{y})}{P_\mathbf{h}^n(\mathbf{y})} \right)^{r_n \frac{w_\mathbf{h}}{M_\mathbf{h}}}$$

- Entropy maximisation (Schaeben):

$$f^{n+1}(g) = f^n(g) \prod_{m=1}^{M_\mathbf{h}} \left(\frac{P_\mathbf{h}(\mathbf{y})}{P_\mathbf{h}^n(\mathbf{y})} \right)^{\frac{r_\mathbf{n}}{M_\mathbf{h}}}$$

- arbitrarily defined cells (ADC, Pawlik): Very similar to E-WIMV, with integrals along path tubes

Layering

Asymmetric Bragg-Brentano

$$C_{\chi}^{\text{top film}} = g_1\left(1-\exp\left(-\mu T g_2/\cos\chi\right)\right)/\left(1-\exp\left(-2\mu T/\sin\omega\cos\chi\right)\right)$$

$$C_{\chi}^{\text{cov. layer}} = C_{\chi}^{\text{top film}}\left(\exp\left(-g_2\sum\mu_i' T_i'/\cos\chi\right)\right)/\left(\exp\left(-2\sum\mu_i' T_i'/\sin\omega\cos\chi\right)\right)$$

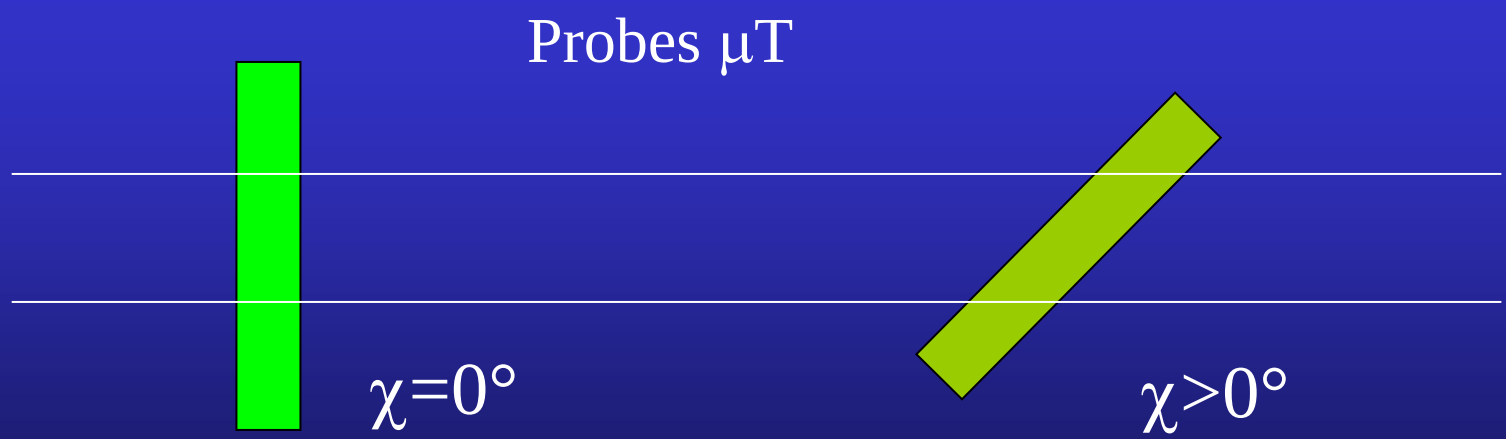

Specular reflectivity: **q**=(0,0,z)

- Fresnel:

$$R(\mathbf{q}) = \left| \frac{q_z - \sqrt{q_z^2 - q_c^2 + \frac{32i\pi^2\beta}{\lambda^2}}}{q_z + \sqrt{q_z^2 - q_c^2 + \frac{32i\pi^2\beta}{\lambda^2}}} \right|^2 \delta q_x \delta q$$

- matrix:

$$R^{flat} = \frac{r_{0,1}^2 + r_{1,2}^2 + 2r_{0,1}r_{1,2}\cos 2k_{Z,1}h}{1 + r_{0,1}^2 r_{1,2}^2 + 2r_{0,1}r_{1,2}\cos 2k_{Z,1}h}$$

- Born approximation:

$$R(q_z) = r.r^* = R_F(q_z)\left| \frac{1}{\rho_s} \int_{-\infty}^{+\infty} \frac{d\rho(z)}{dz} e^{iq_z z} dz \right|^2$$

- Roughness:

$$R^{rough}(q_z) = R(q_z)\exp(-q_{z,0}q_{z,1}\sigma^2) \quad \text{Low-angles (reflectivity)}$$

$$S_R = 1 - p\exp(-q) + \mathrm{p}\exp\left(\frac{-\mathrm{q}}{\sin\theta}\right) \quad \text{high-angle (Suortti)}$$

Strain-Stress

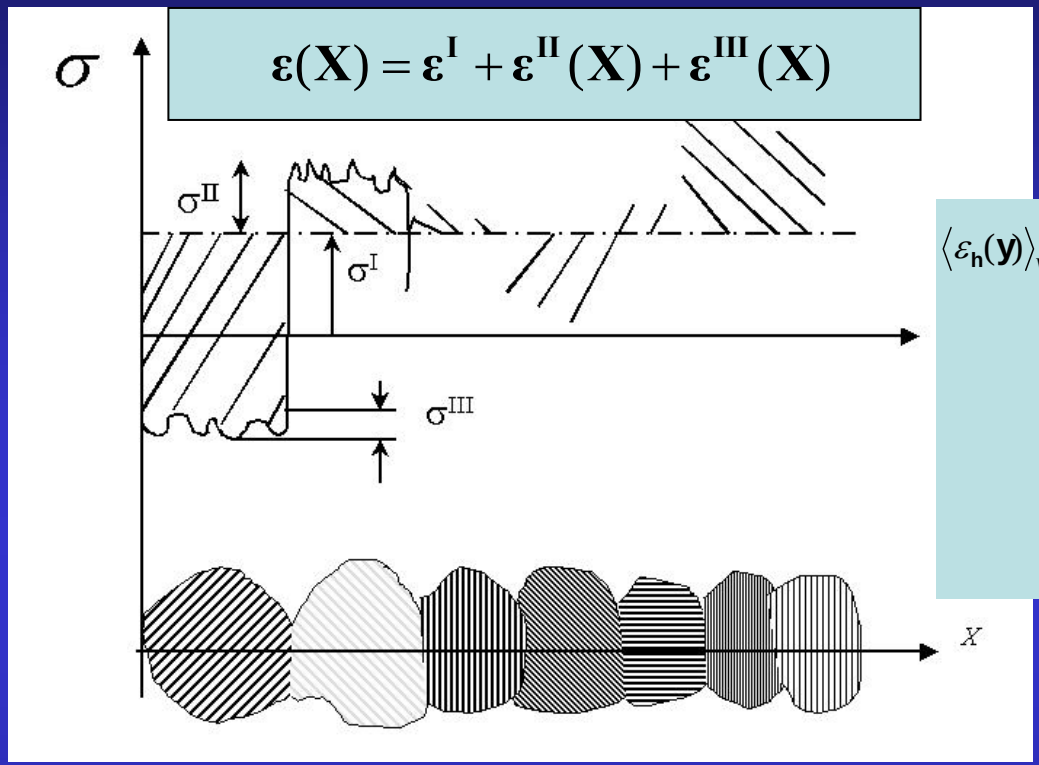

$$\boldsymbol{\varepsilon}(\mathbf{X}) = \boldsymbol{\varepsilon}^{\mathbf{I}} + \boldsymbol{\varepsilon}^{\mathbf{II}}(\mathbf{X}) + \boldsymbol{\varepsilon}^{\mathbf{III}}(\mathbf{X})$$

Isotropic samples:
triaxial, biaxial uniaxial stress state

$$\begin{aligned}\left\langle \varepsilon_{\mathbf{h}}(\mathbf{y}) \right\rangle_{V_d} &= \frac{1}{V_d}\int_{V_d}(\varepsilon_{33}^{I}+\varepsilon_{33}^{II}+\varepsilon_{33}^{III})dV \\ &= (\varepsilon_{11}^{I}\cos^2\phi+\varepsilon_{12}^{I}\sin 2\phi+\varepsilon_{22}^{I}\sin^2\phi-\varepsilon_{33}^{I})\sin^2\psi+\varepsilon_{33}^{I}+ \\ &(\varepsilon_{13}^{I}\cos\phi+\varepsilon_{23}^{I}\sin\phi)\sin 2\psi+\frac{1}{V_d}\int_{V_d}(\varepsilon_{33}^{IIe}+\varepsilon_{33}^{IIti}+\varepsilon_{33}^{IIpi})dV \\ &= \frac{\left\langle d(hkl,\phi,\psi)\right\rangle_{V_d}-d_0(hkl)}{d_0(hkl)}\end{aligned}$$

Textured samples:
triaxial, biaxial uniaxial stress state
+ ODF + SDF + model

$$\chi^2 = \sum_i w_i^{\,2}\left[\varepsilon_i^{calc}(S_{ijk\ell}^{M},\mathbf{h},\mathbf{y}) - \varepsilon_i^{meas}(S_{ijk\ell}^{M},\mathbf{h},\mathbf{y})\right]^2$$

Non-linear least-square fit

$$\begin{aligned}\left\langle E(\mathbf{g}) \right\rangle_{V_d} &= \frac{1}{V_d}\int_{V_d} E^{SC}(g)\,f(g)dg \\ &= \left(\prod_{V_d} E^{SC}(g)\,f(g)dg\right)^{\frac{1}{V_d}}\end{aligned}$$

Phase analysis

- Volume fraction

$$V_\Phi = \frac{S_\Phi V_{uc\Phi}^2}{\sum_\Phi \left(S_\Phi V_{uc\Phi}^2\right)_\Phi}$$

- Weight fraction

$$m_\Phi = \frac{S_\Phi Z_\Phi M_\Phi V_{uc\Phi}^2}{\sum_\Phi \left(S_\Phi Z_\Phi M_\Phi V_{uc\Phi}^2\right)_\Phi}$$

Z = number of formula units

M = mass of the formula unit

V = cell volume

Implemented codes

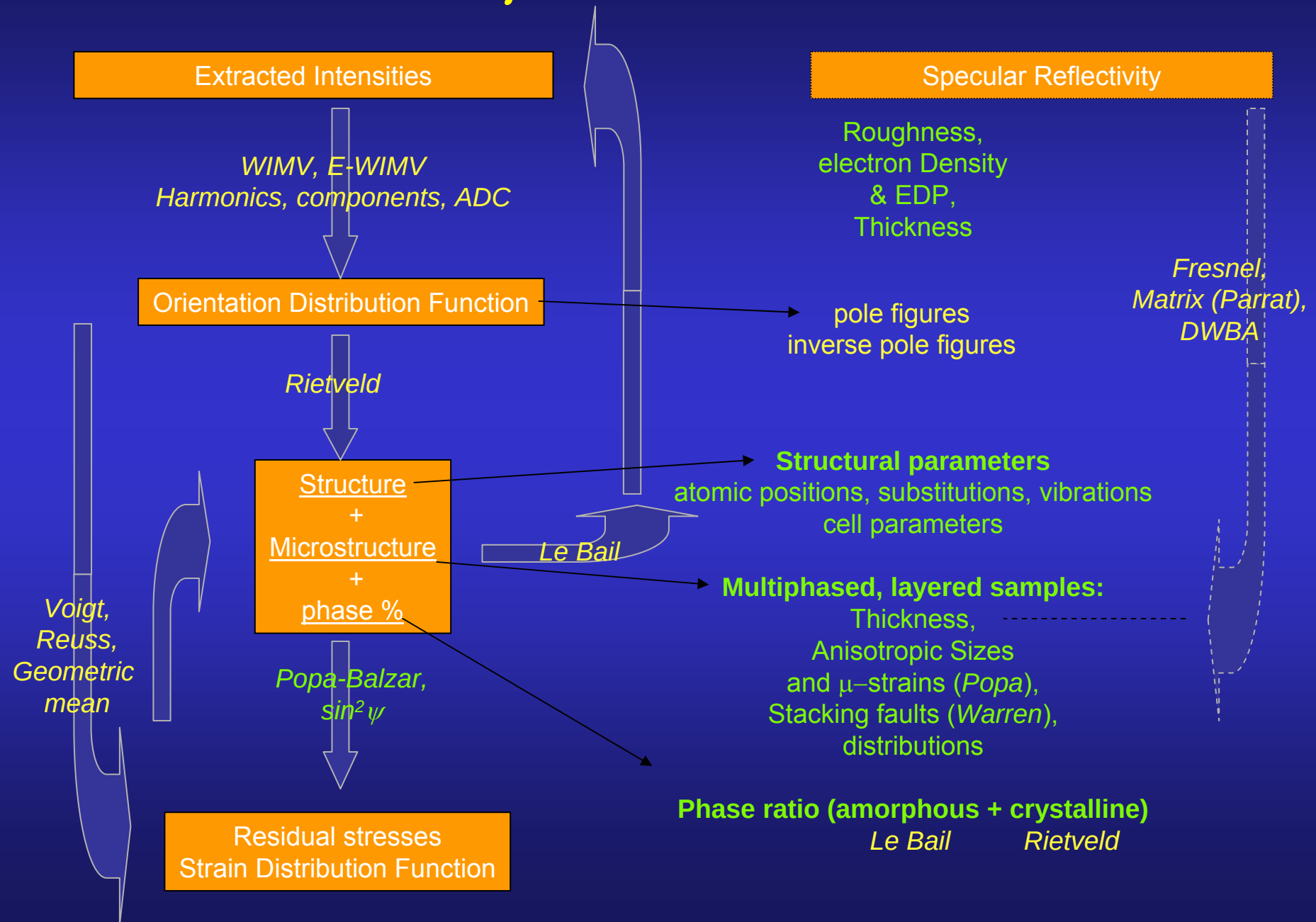

Minimum experimental requirements

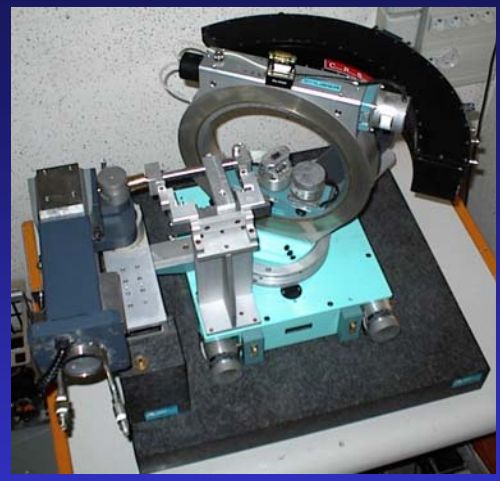

1D or 2D Detector + 4-circle diffractometer
(X-rays and neutrons)
CRISMAT, ILL

+

~1000 experiments (2θ diagrams)
in as many sample orientations

+

Instrument calibration
(peaks widths and shapes,
misalignments, defocusing …)

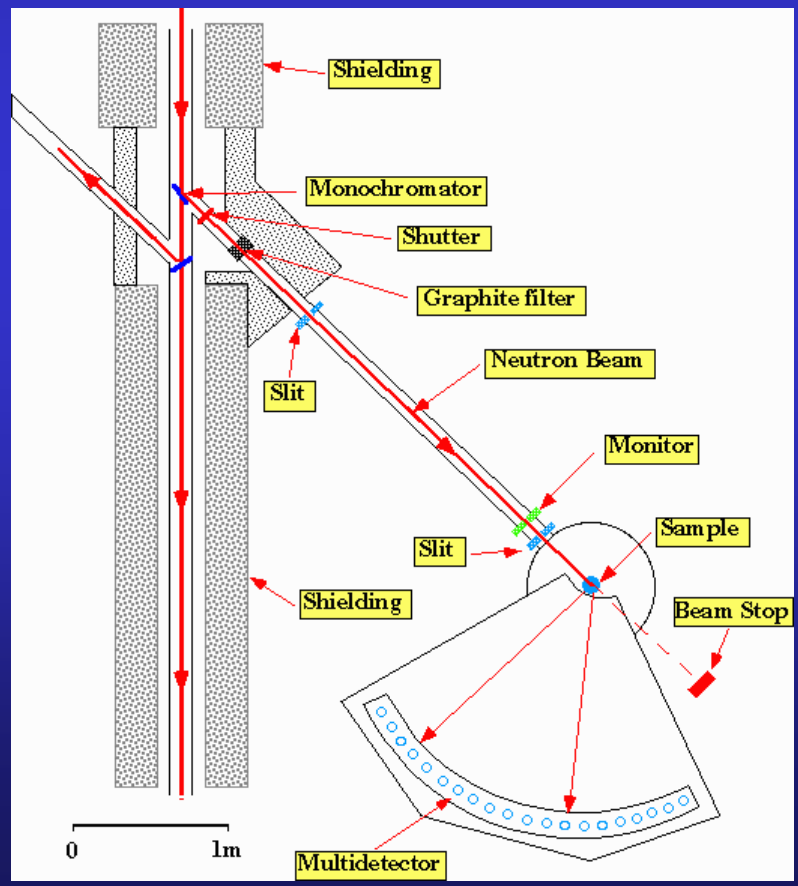

Calibration

ω = 20°

60°

χ

0°

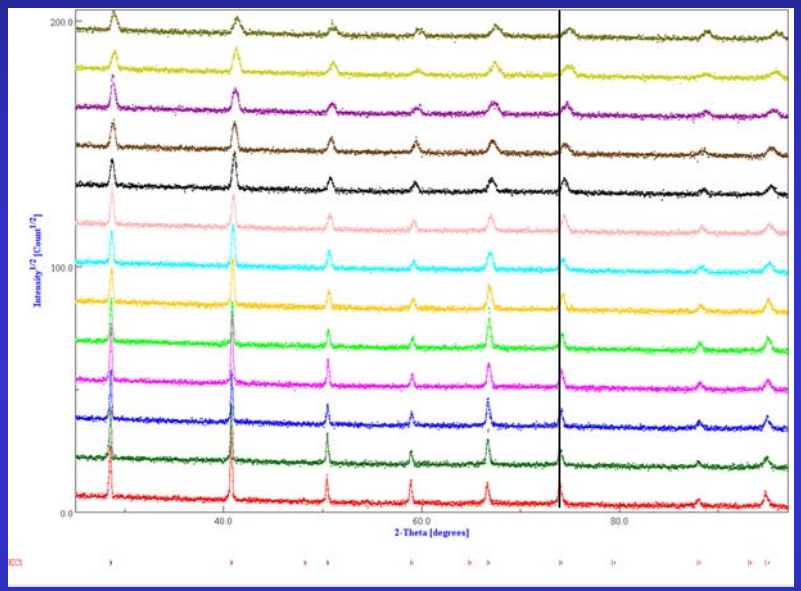

ω = 40°

60°

χ

0°

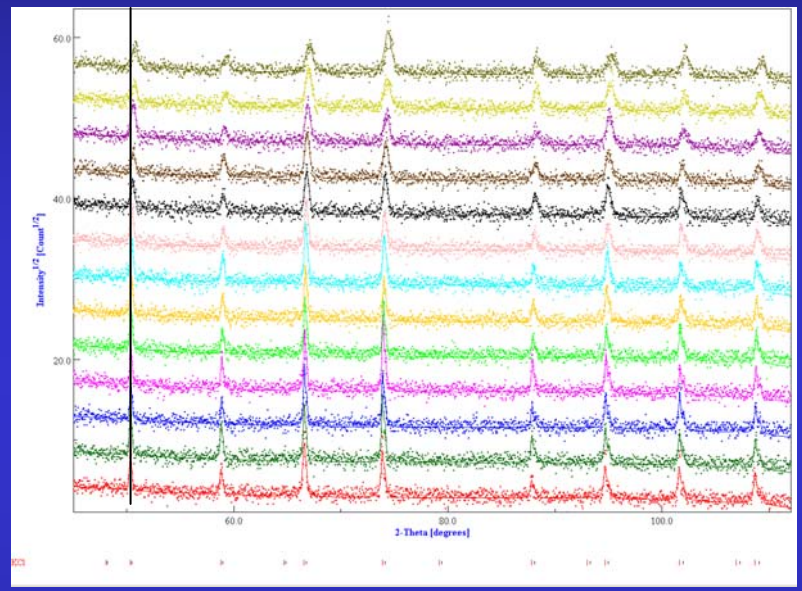

KCl, LaB_6 …

FWHM (ω, χ, 2θ …)
2θ shift
gaussianity
asymmetry
misalignments ...

Methodology implementation

L. Lutterotti, Trento

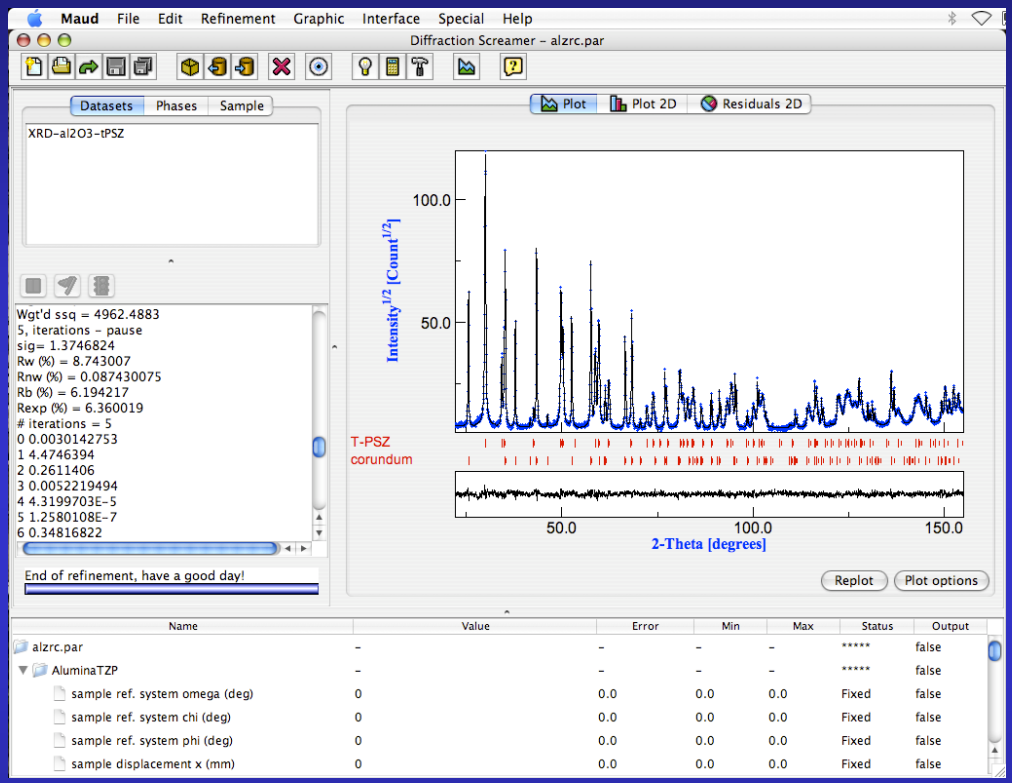

User friendly interface

Java codes

Java web start updates

Bi2223 compounds

E. Guilmeau, PhD

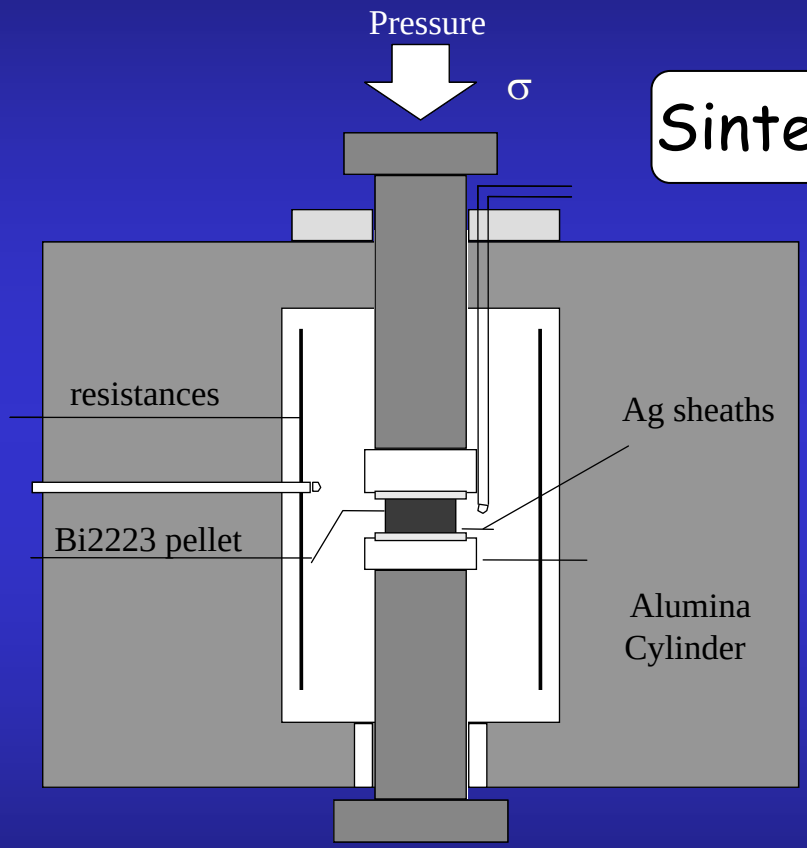

Sinter-Forging

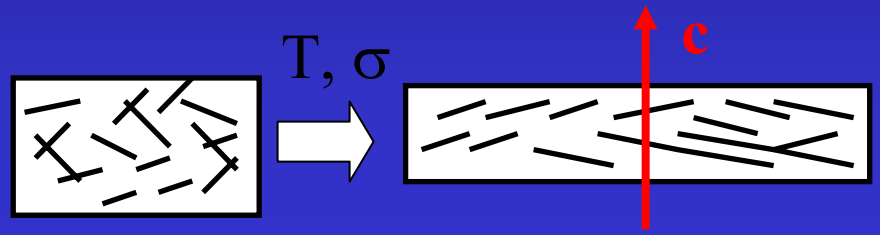

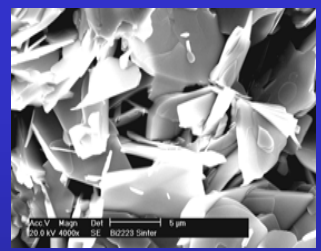

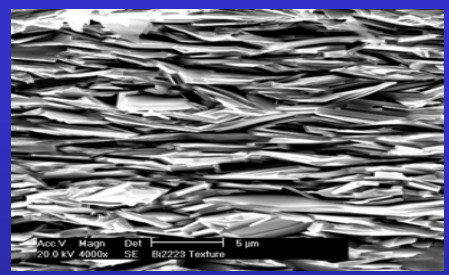

Grain alignment ⇒ ↗Jc

(00ℓ) Texture

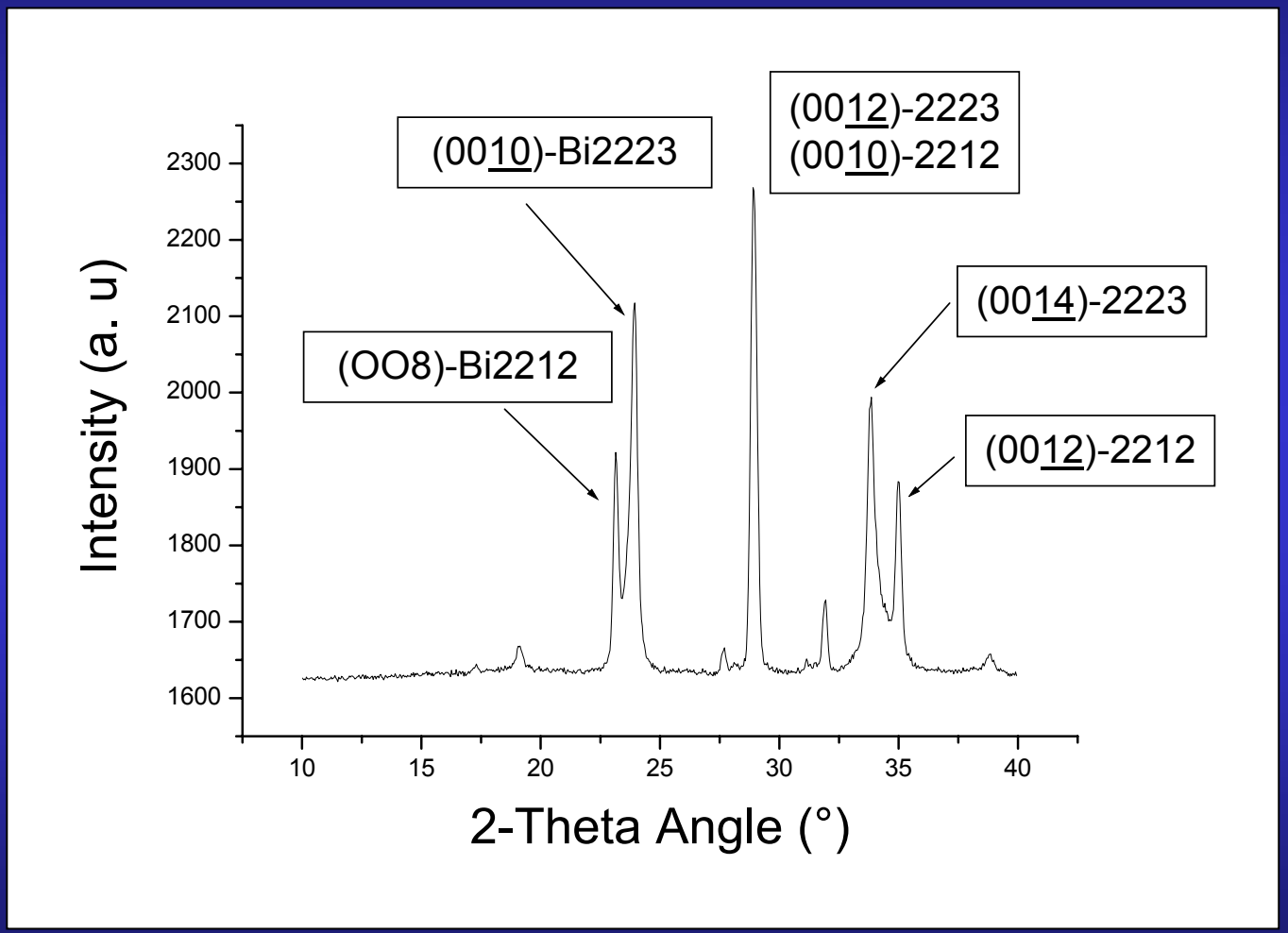

Bi2212 + Secondary phases ⟶ Bi2223

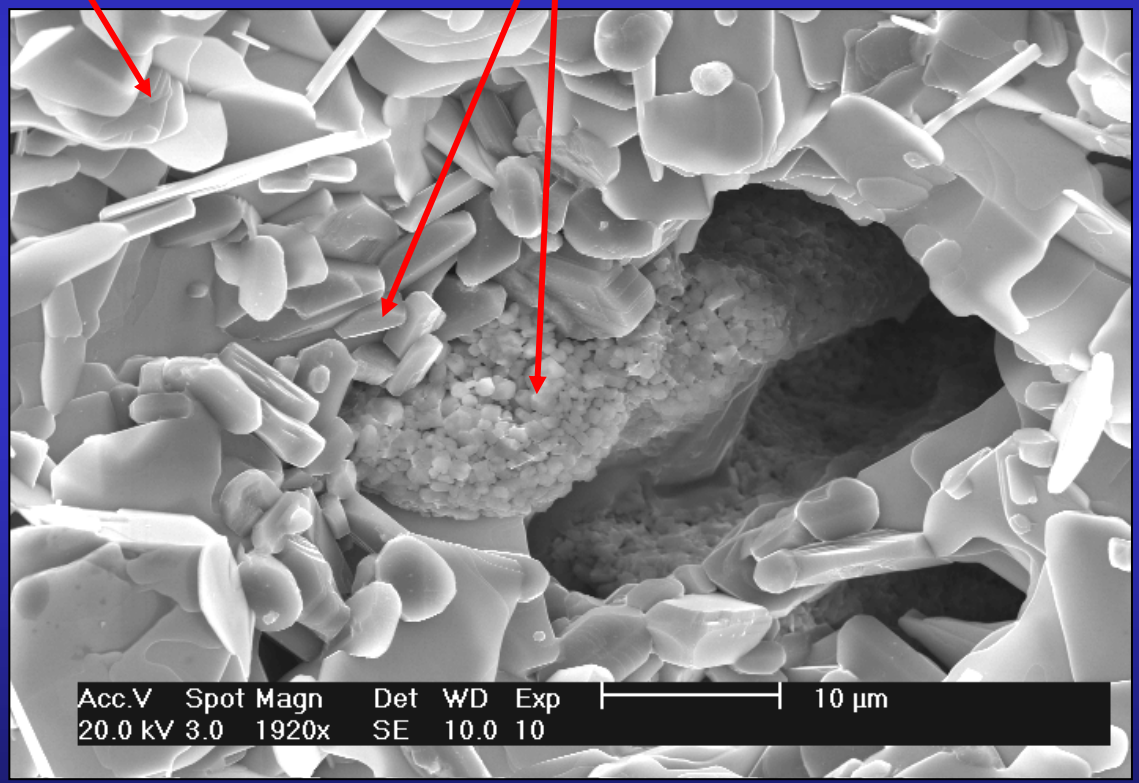

Combined Analysis

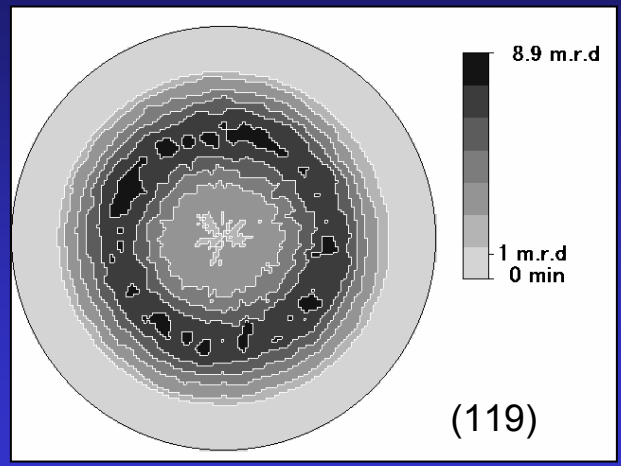

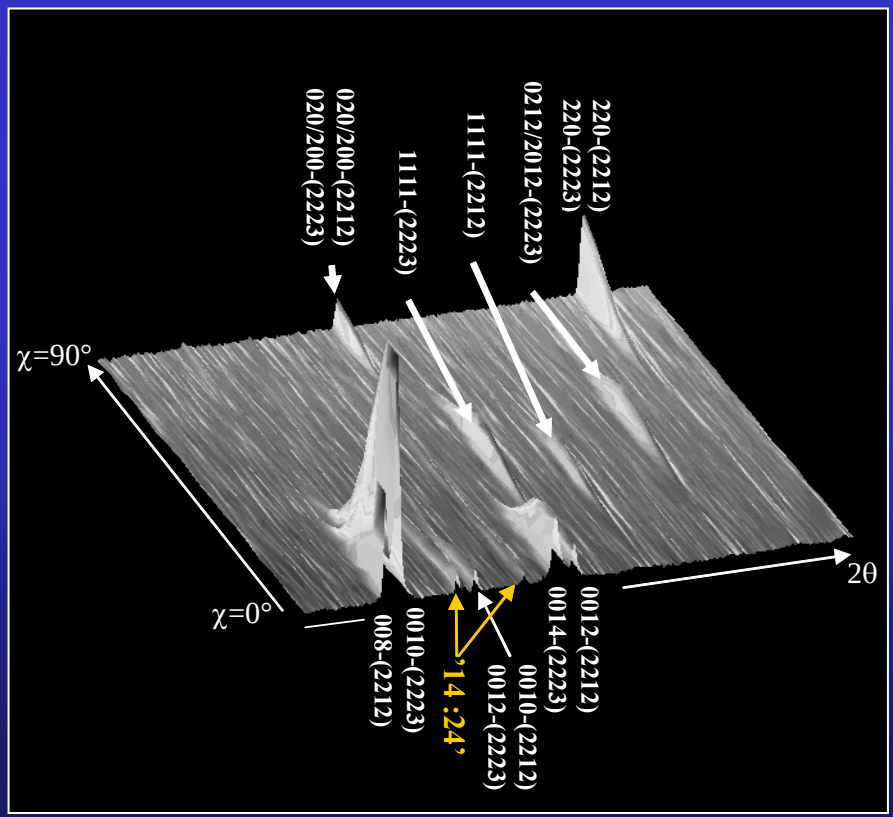

-Neutrons

-Sample: ~70 mm^3

-2θ patterns for χ=0° to 90°

-No φ rotation (fibre texture).

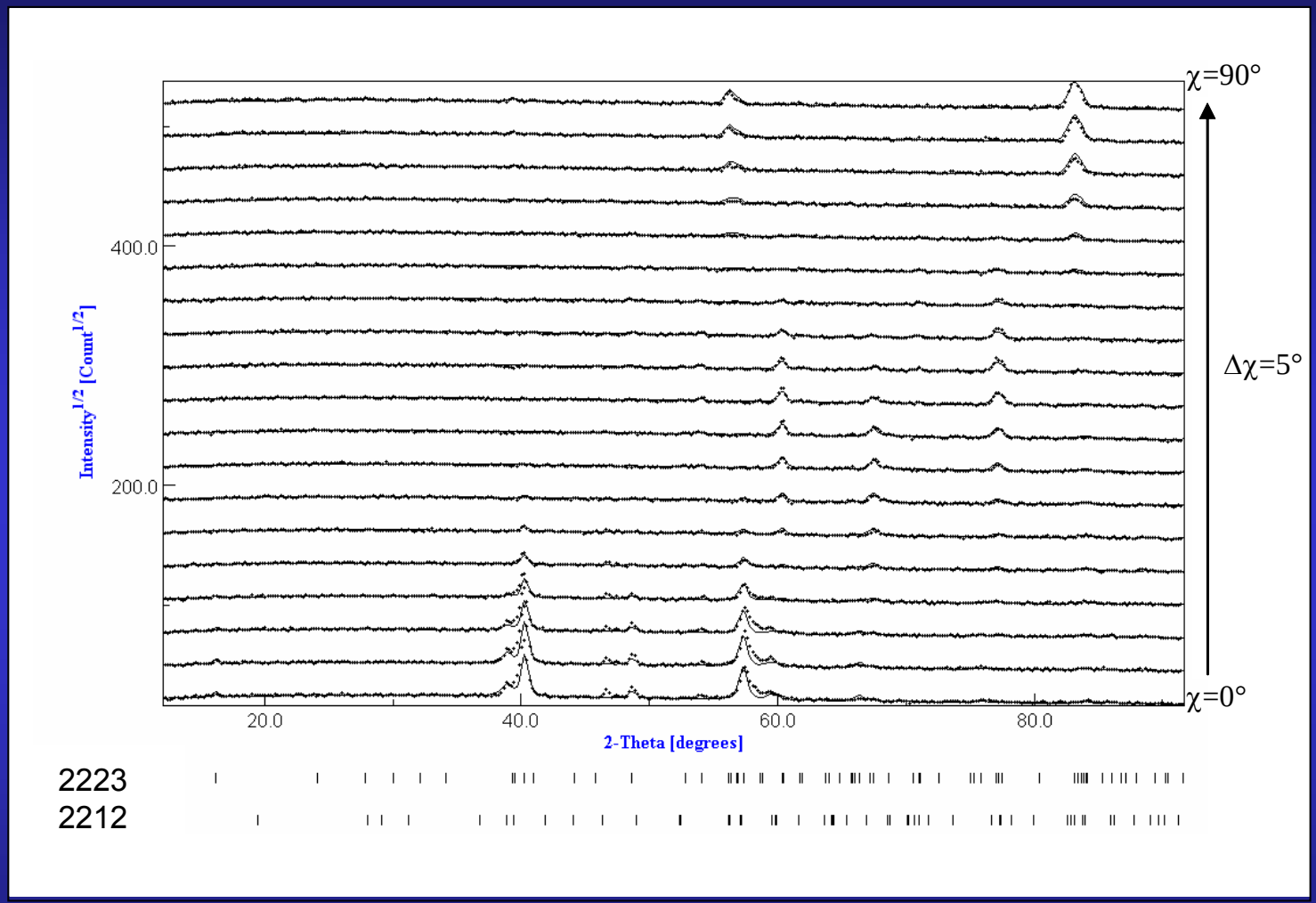

Rw=9.12
RP=16.24

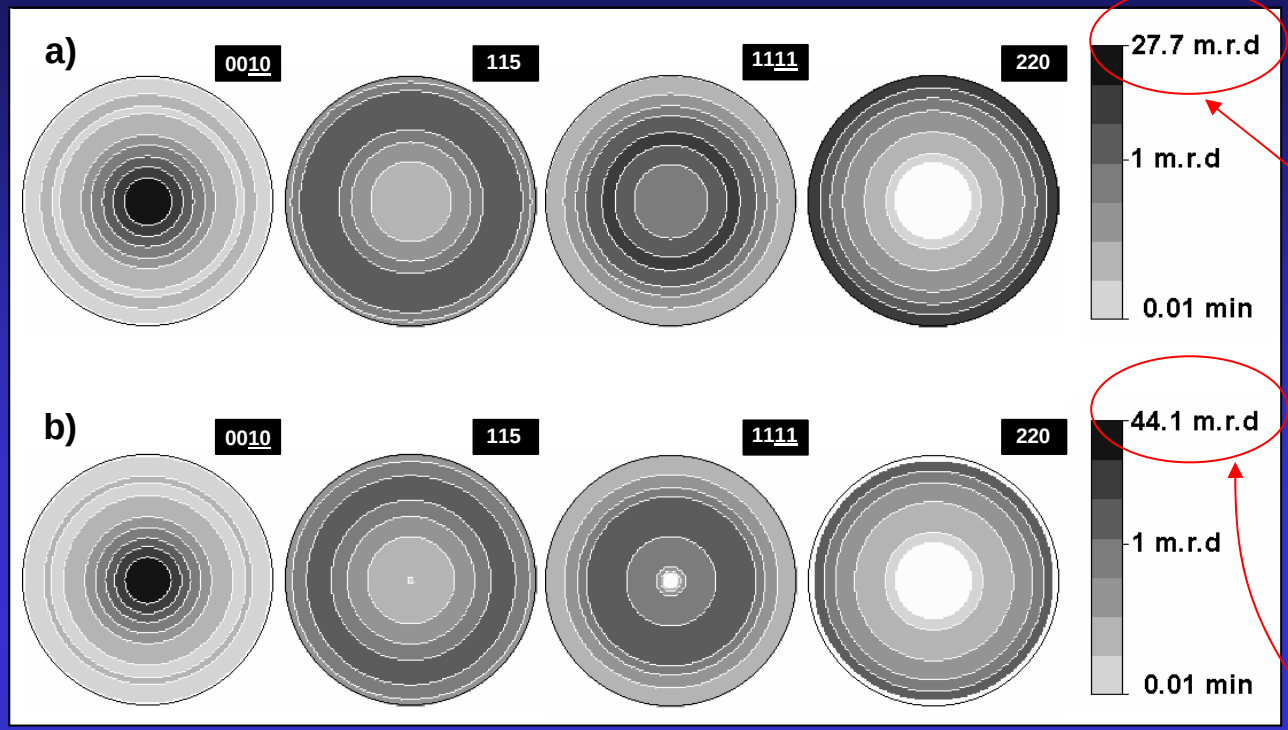

Logarithmic density scale, equal area projection

Recalculated (WIMV)

Extracted (Le Bail)

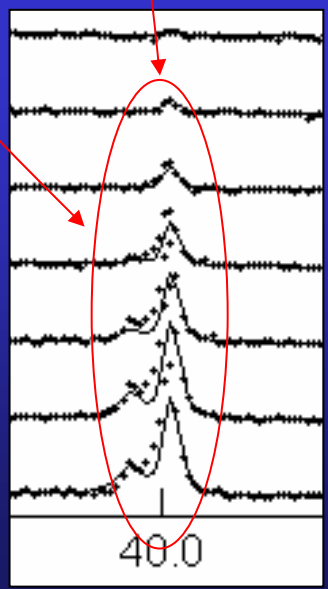

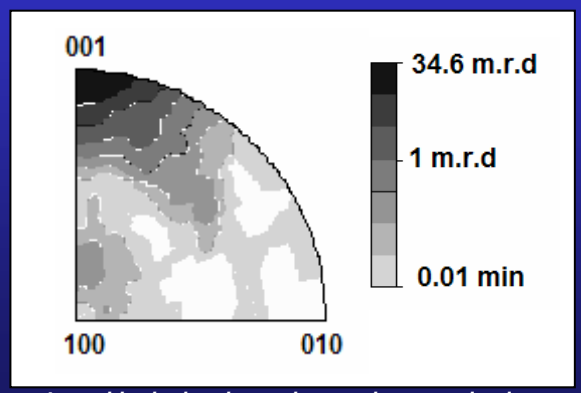

Logarithmic density scale, equal area projection

Stacking faults and/or intergrowth on the c-axis →New periodicities and peaks characterized with intermediate c parameters.

However, no algorithm is included to solve intergrowths in the combined approach.

Effect of the sinter-forging treatment on the texture development, crystal growth, transport properties

Sinter-forging dwell time (h)	*Orientation Distribution Max (m.r.d.)*		*% Bi2223*	*Cell parameters (Å)*		*Crystallite size Bi2223 (nm)*	*Rb (%)*	*Rw (%)*	*Rexp (%)*	*RP0 (%)*	*RP1 (%)*	*J_c (A/cm²)*
	Bi2212	*Bi2223*		*Bi2223*	*Bi2212*							
20	21.8	20.7	59.9±1.3	a=5.419(3) b=5.391(3) c=37.168(3)	a=5.414(3) b=5.393(3) c=30.800(3)	205±7	7.56	11.1	4.55	17.74	10.56	12500
50	24.1	24.4	72.9±2.9	a=5.419(3) b=5.408(3) c=37.192(3)	a=5.416(3) b=5.396(3) c=30.806(3)	273±10	7.54	11.37	4.58	17.05	11.04	15000
100	31.5	25.2	84.4±4.6	a=5.410(3) b=5.405(3) c=37.144(3)	a=5.412(3) b=5.403(3) c=30.752(3)	303±10	5.4	8.04	3.69	13.54	9.31	19000
150	65.4	27.2	87.0±4.1	a=5.417(3) b=5.403(3) c=37.199(3)	a=5.413(3) b=5.407(3) c=30.792(3)	383±13	6.13	9.12	4.8	16.24	12.25	20000

E. Guilmeau et al., JAC

$Ca_3Co_4O_9$ thermoelectrics

J.G. Noudem, Caen

$Ca_3Co_4O_9$: Misfit lamellar and modulated Structure, with high thermopower

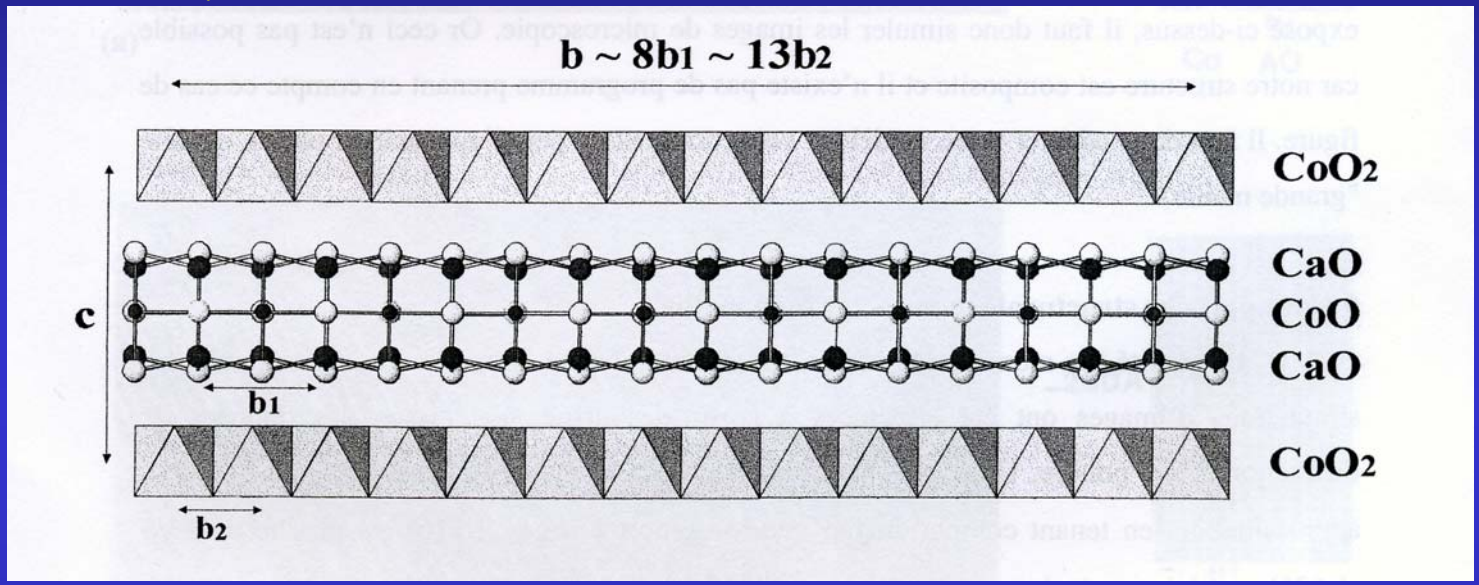

Two monoclinic sub-systems:

S1 with a ~ 4.8Å, b_1 ~ 4.5Å, c ~ 10.8Å et β ~ 98° (NaCl-type)

S2 with a ~ 4.8Å, b_2 ~ 2.8Å, c ~ 10.8Å et β ~ 98° (CdI_2-type)

$\Gamma=\sigma_{ab}/\sigma_c$~10 ⇒ Texture

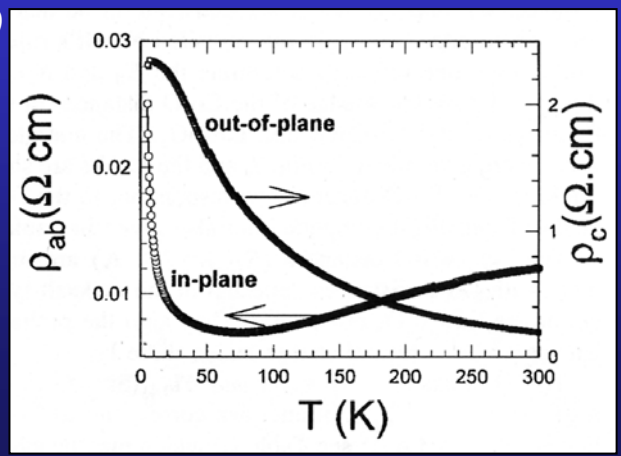

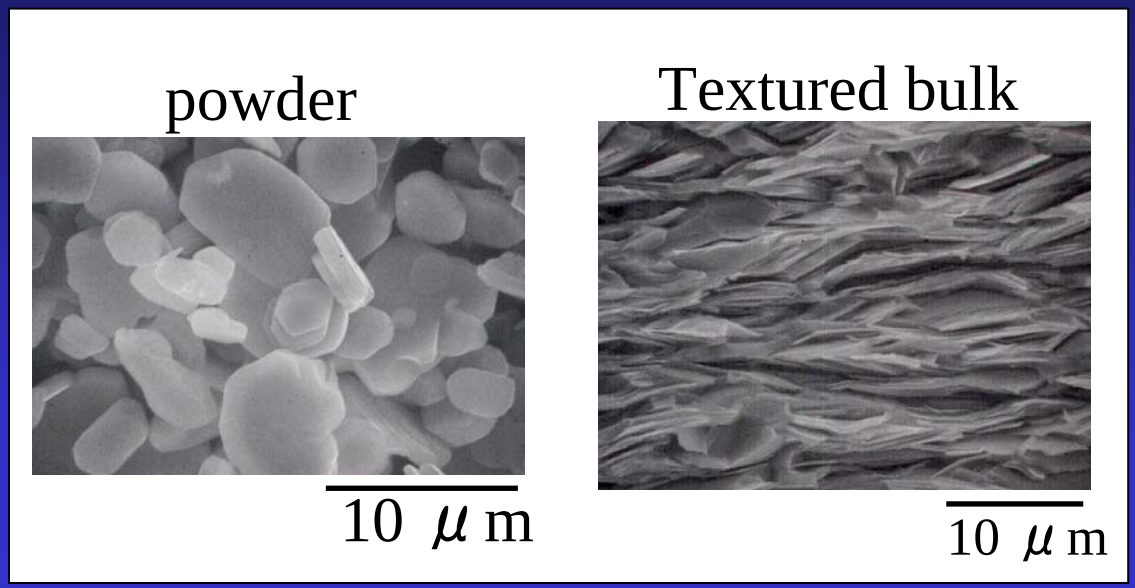

Magnetic alignment and Templated Growth method

Analysis:

- neutrons

- 3D Supercell: a=4.8309Å, b~8b1~13b2~36.4902Å, c=10.8353Å, β=98.13°

174 atoms/cell

-Sample : 0.6 cm^3

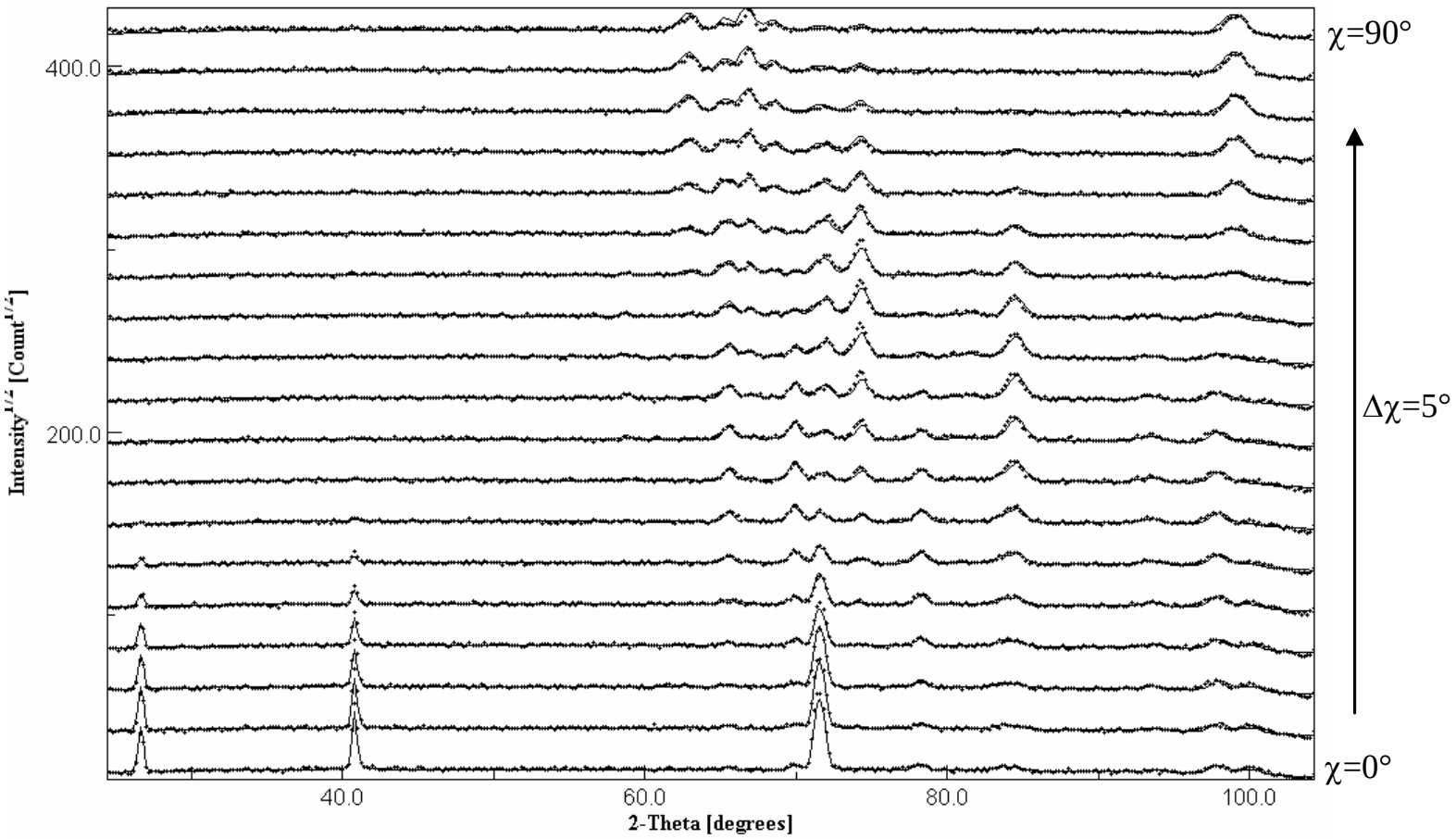
χ=90°
400.0
200.0
Intensity$^{1/2}$ [Count$^{1/2}$]
Δχ=5°
χ=0°
40.0
60.0
80.0
100.0
2-Theta [degrees]
Supercell

RP=19.7%, Rw=11.9%

9.8 MPa for 2 h

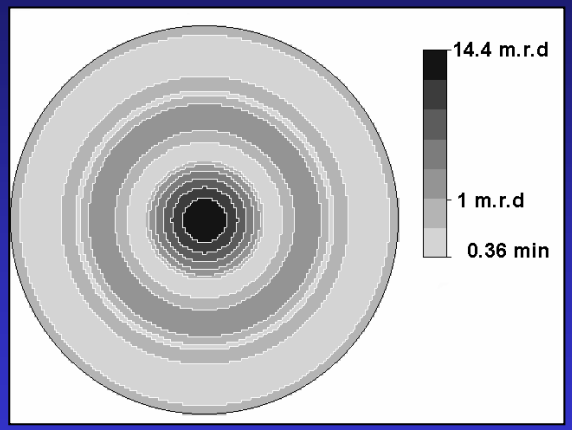

19.6 MPa for 6 h

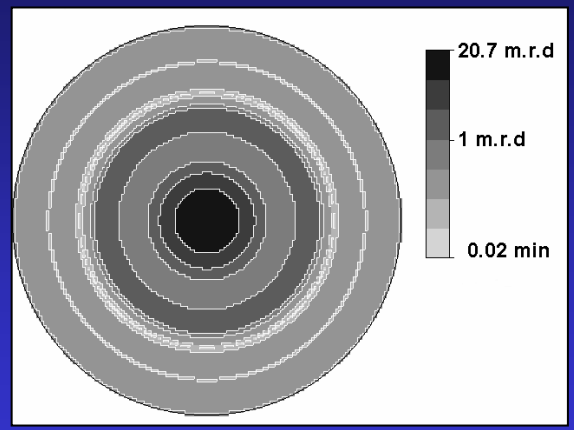

19.6 MPa for 20 h

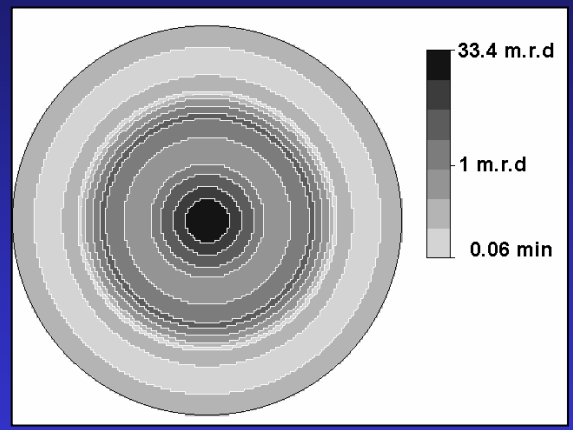

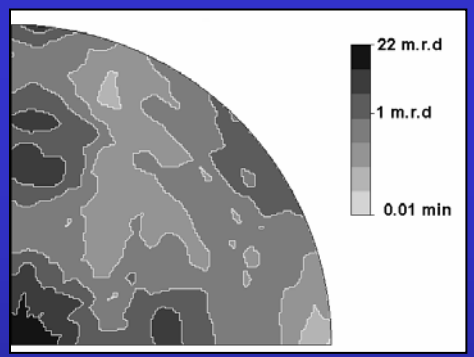

Templated Growth Method

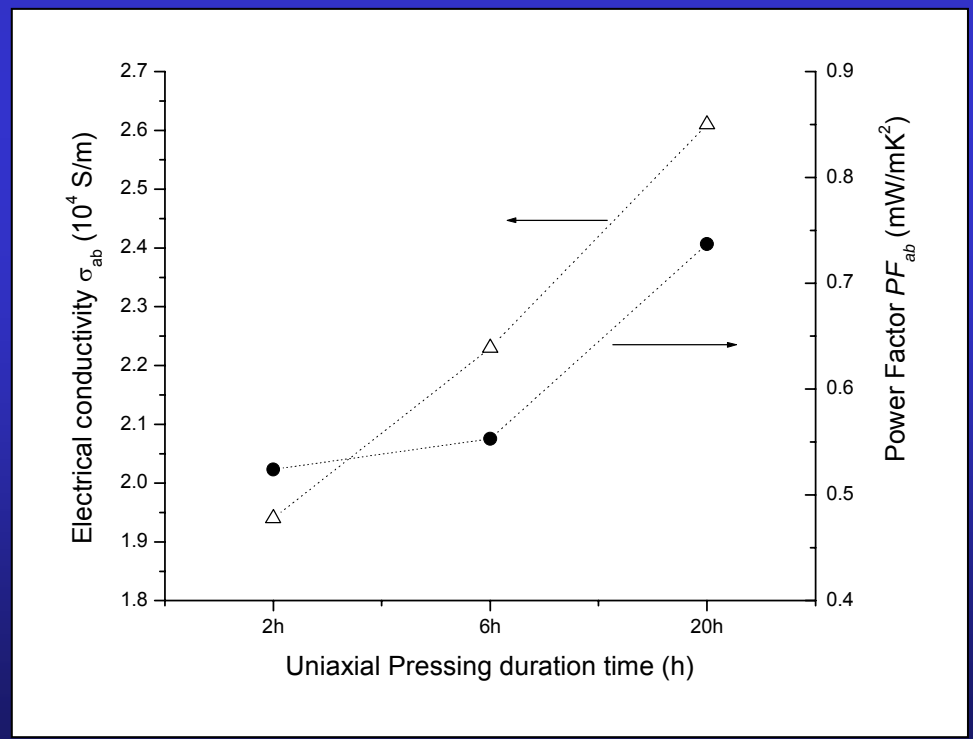

Magnetic Alignment

Logarithmic density scale, equal area projection

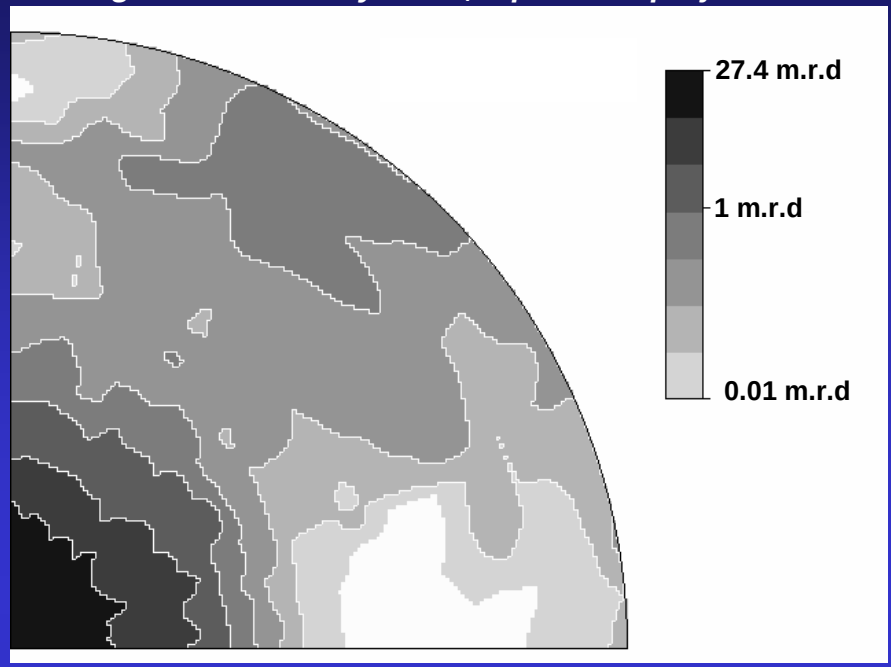

- magnetic alignment really efficient to obtain strong textures
- combined analysis of modulated structures possible

Ferroelectric PCT films

J. Ricote, Madrid

thin films:

$(Ca_{0.24}Pb_{0.76})TiO_3$ sol-gel synthesised solutions deposited by spin coating on a substrate of $Pt/TiO_2/Si$, with and without a treatment at 650ºC for 30 min.

All films are crystallised at 700ºC for 50 s by Rapid Thermal Processing (RTP; 30ºC/s). A series is also recrystallised at 650ºC for 1 to 3 h.

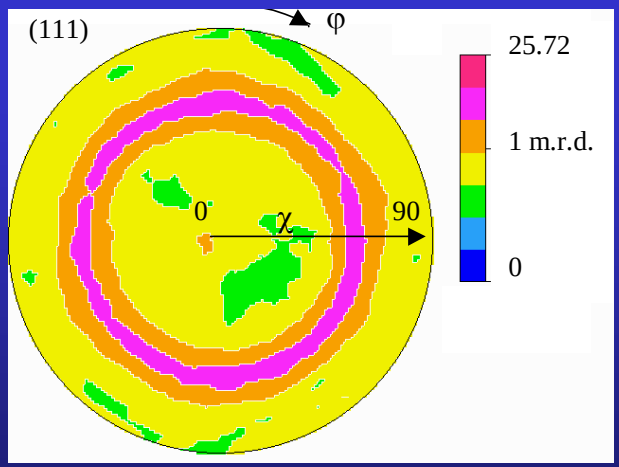

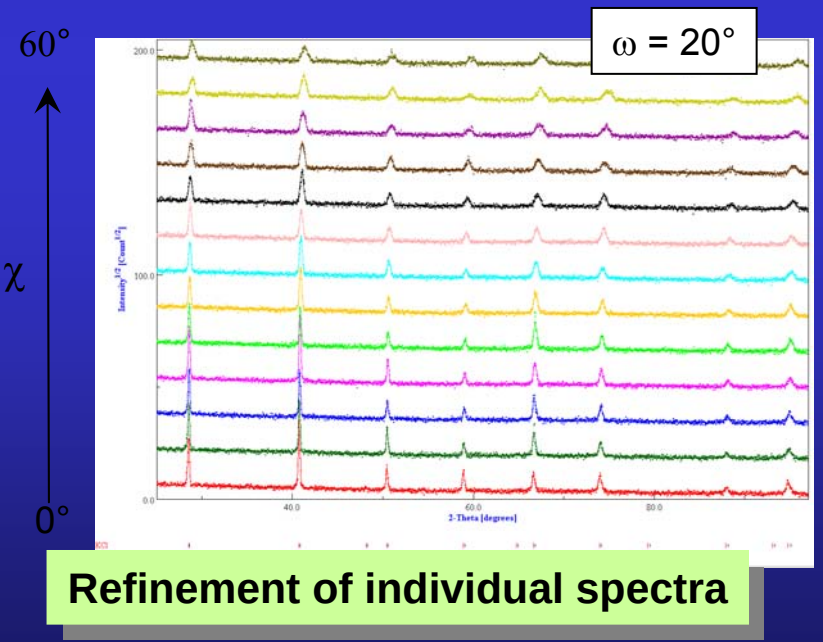

Refinement of individual spectra

Limitations of the simple Quantitative Texture Analysis

Structural parameters are difficult to obtain due to:

Substrate influence:
overlapping of reflections from the film and the substrate

TEXTURE effects:
peaks that do not appear at low χ angles

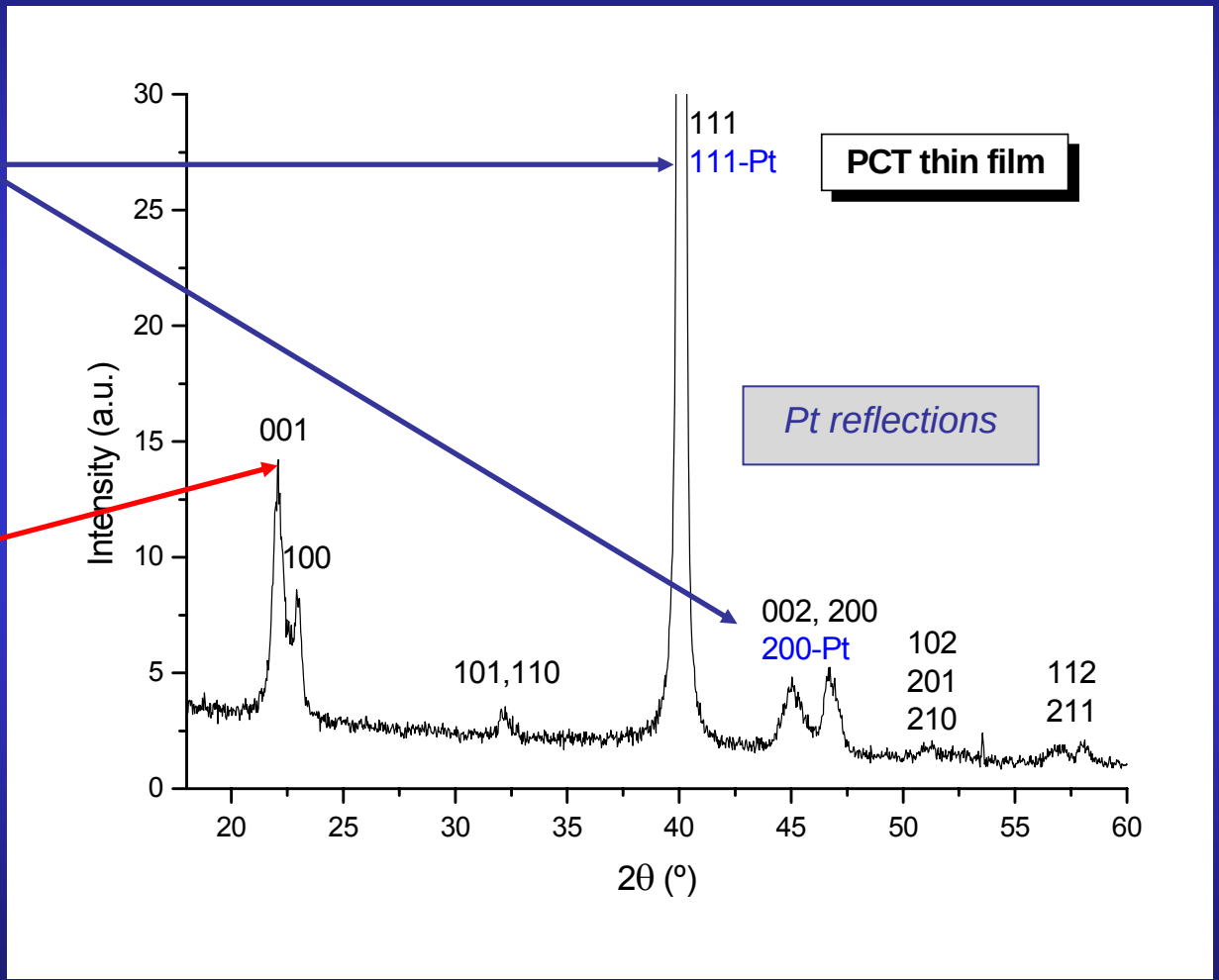

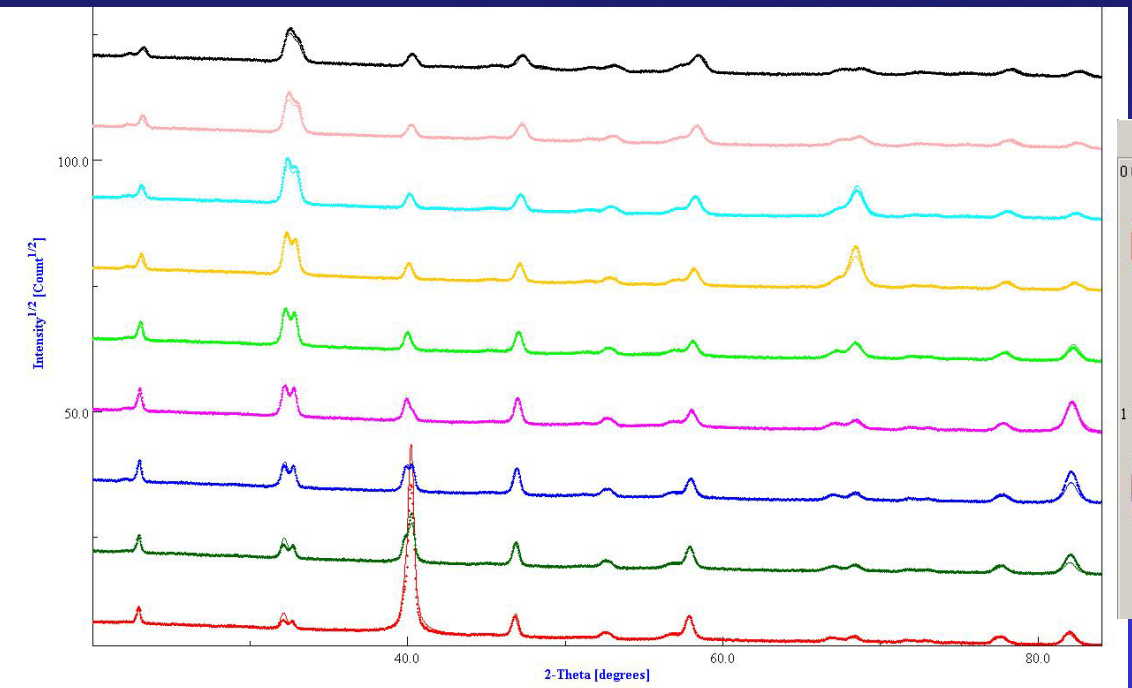

PCT

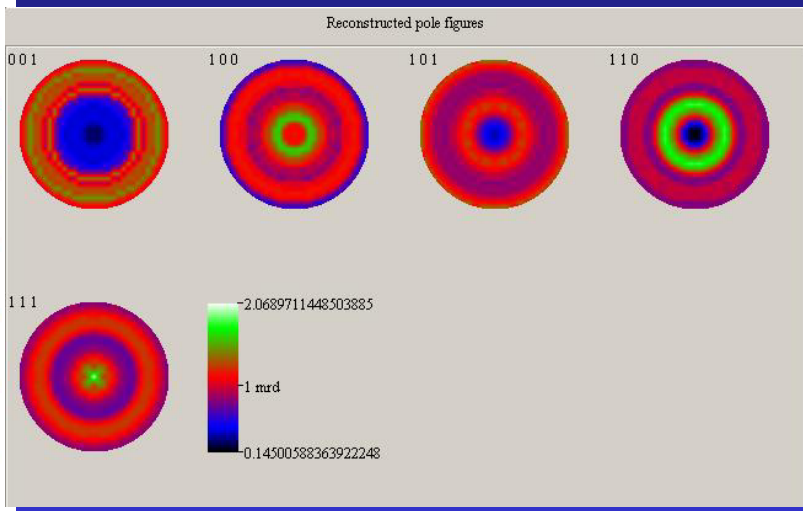

a = 3.9156(1) Å
c = 4.0497(3) Å
T = 2525(13) Å
t_{iso} = 390(7) Å
ε = 0.0067(1) rms

Pt

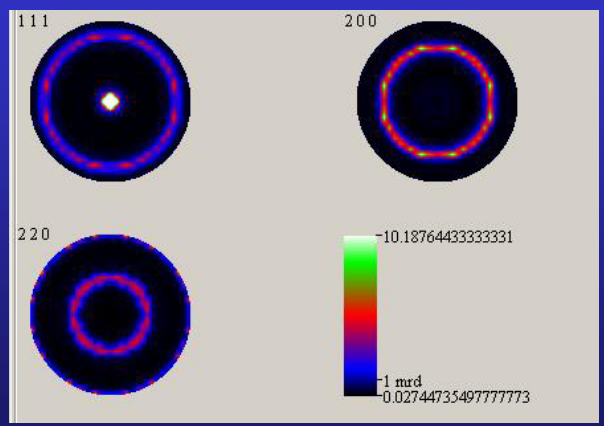

a = 3.9108(1) Å
T = 457(3) Å
t_{iso} = 458(3) Å
ε' = 0.0032(1) rms

R_W = 13%; R_B = 12%; R_{exp} = 22%.(Rietveld)
R_W = 5%; R_B = 6% (E-WIMV)

Atom	Occupancy	x	y	z
Pb	0.76	0.0	0.0	0.0
Ca	0.24	0.0	0.0	0.0
Ti	1.0	0.5	0.5	0.477(2)
O1	1.0	0.5	0.5	0.060(2)
O2	1.0	0.0	0.5	0.631(1)

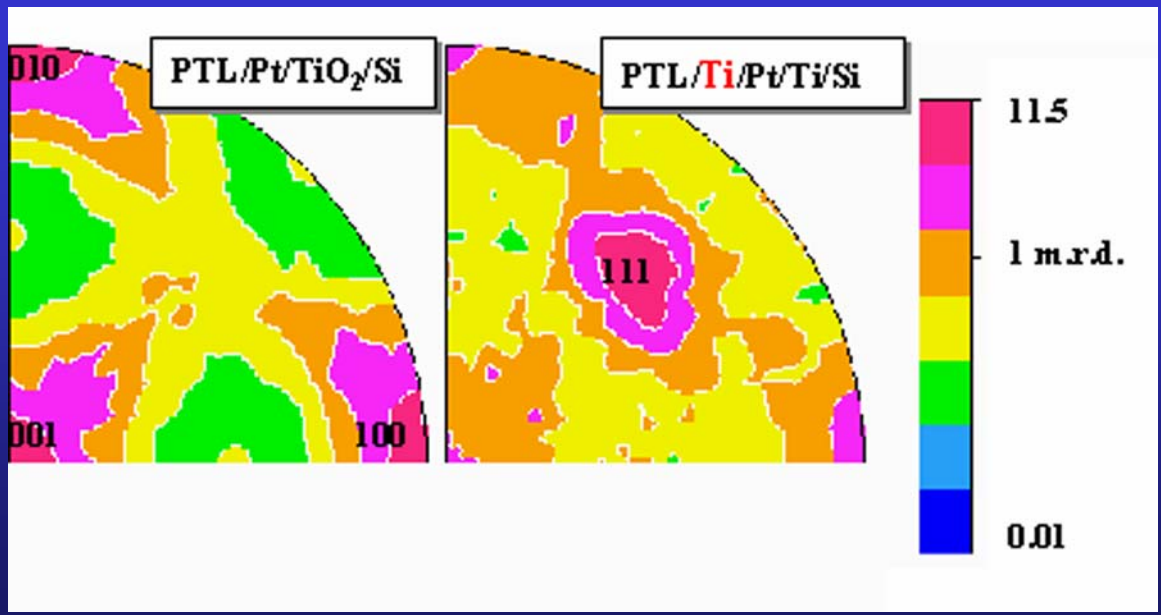

Structural parameters

Pt layer

	a (Å)	thickness (nm)	R factors (%)
non-treated substrate			
Pt	3.9108(1)	45.7(3)	R_W=13, R_B=12, R_{exp}=22
annealed substrate			
Pt	3.9100(4)	46.4(3)	R_W=8, R_B=14, R_{exp}=21
Pt (Recryst. 1h)	3.9114(2)	47.8(3)	R_W=9, R_B=20, R_{exp}=21
Pt (Recryst. 2h)	3.9068(1)	46.9(3)	R_W=9, R_B=14, R_{exp}=22
Pt (Recryst. 3h)	3.9141(4)	47.5(9)	R_W=27, R_B=12, R_{exp}=21

Annealing of the substrate does not introduce significant variations on the structure of the Pt layer

PTC film

	a (Å)	c (Å)	thickness (nm)
on non-treated substrate			
PCT	3.9156(1)	4.0497(6)	272.5(13)
on annealed substrate			
PCT	3.8920(6)	4.0187(8)	279.0(9)
PCT (Recryst. 1h)	3.8929(2)	4.0230(4)	266.1(11)
PCT (Recryst. 2h)	3.8982(2)	4.0227(4)	258.4(9)
PCT (Recryst. 3h)	3.9001(4)	4.0228(11)	253.6(29)

Recrystallisation reduces the stress on the film, and, increases the lattice parameters

Structural, microstructural and texture quantitative characterisation of ferroelectric thin films by the combined method

Analysis of the X-ray diffraction diagrams of a PCT film on $Pt/TiO_2/Si$

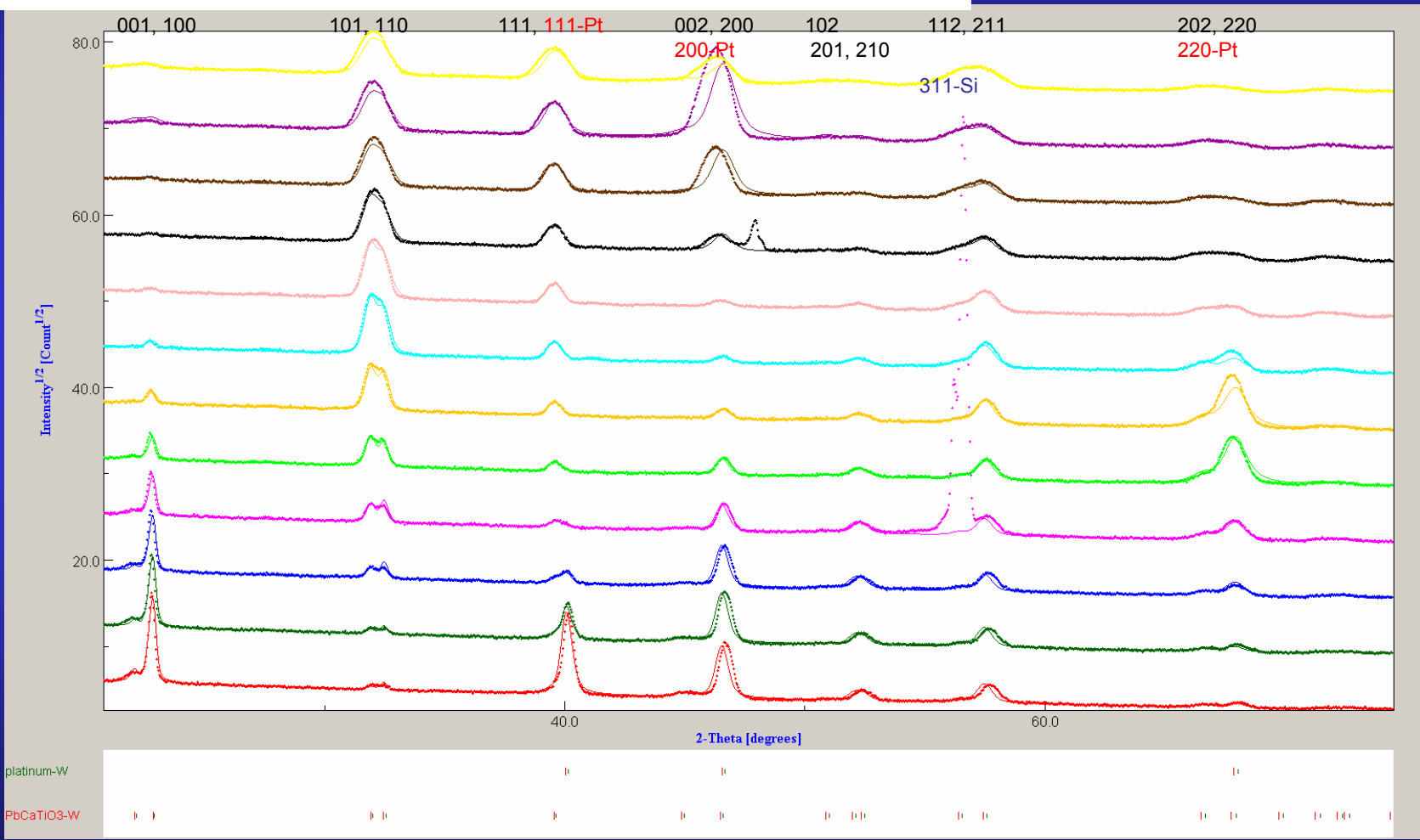

R_W = 13%; R_B = 12%; R_{exp} = 22%.(Rietveld)
R_W = 5%; R_B = 6% (E-WIMV)

Substrate influence on Residual Stress and Texture

Tensile stress

PCT on $Pt/TiO_2/(100)Si$

PCT on $Pt/(100)MgO$

PCT on $Pt/(100)SrTiO_3$

Compressive stress

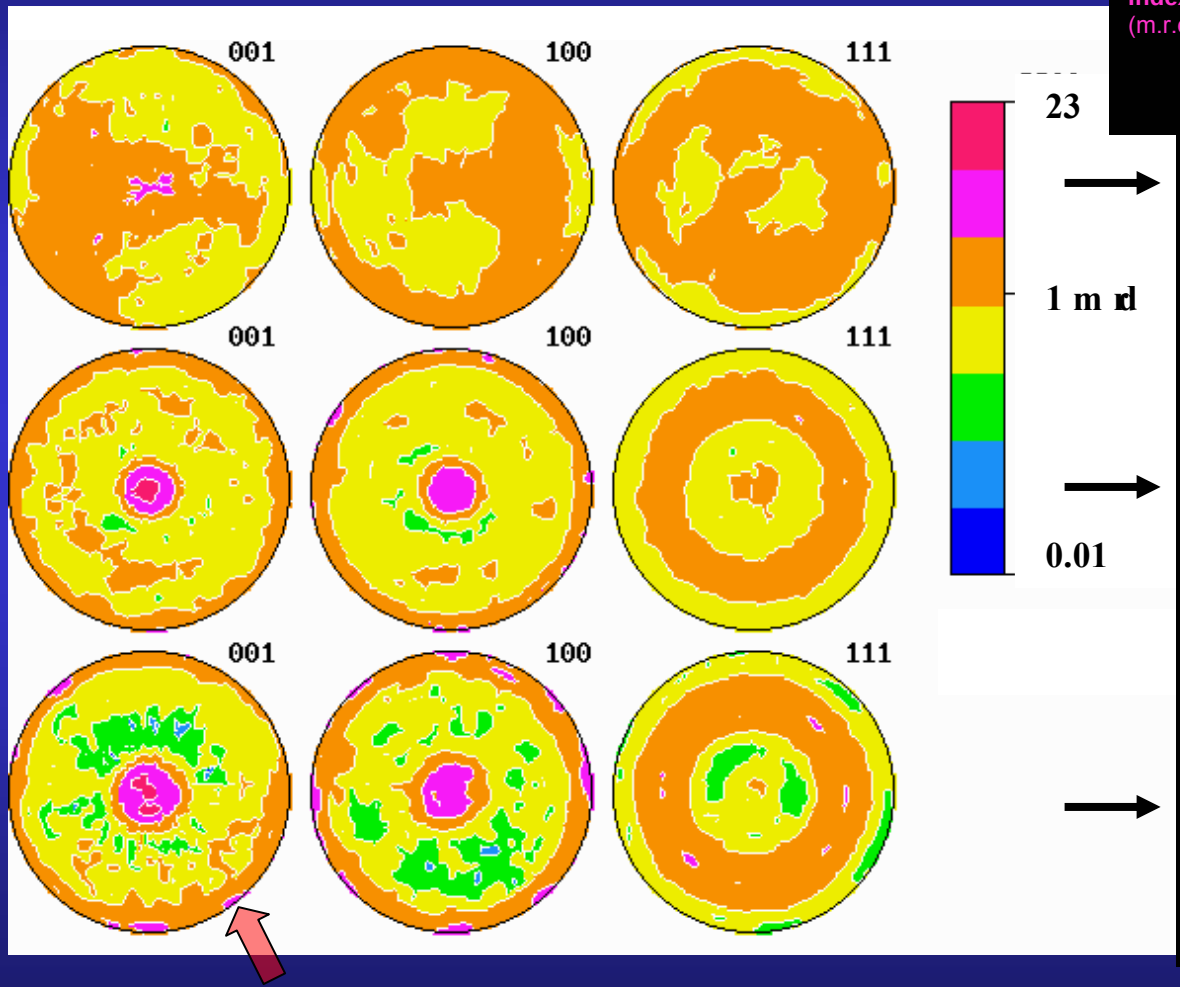

Texture Index (m.r.d.^{2})	Pyroelectric Coefficient (10^{-8}C cm^{-2} K^{-1})
2.1	0.3
5.1	1.5
7.9	1.1

Enhancement of <001> texture

Compliance coefficients [10^{-3} GPa^{-1}]	$PbTiO_3$ single crystal (data set A)	Film random orientation	PCT-Si <001> contrib≈17%	PLT <001> contrib.≈49%	PCT-Mg <001> contrib.≈68%
s_{11}	6.5	10.1	10.5	10.0	9.7
s_{22}	6.5	10.0	10.5	10.0	9.7
s_{33}	33.3	9.8	9.0	10.3	11.3
s_{44}	14.5	13.2	12.8	12.9	13.1
s_{55}	14.5	13.2	12.8	13.0	13.1
s_{66}	9.6	13.4	14.0	13.5	12.7
s_{12}	-0.35	-3.3	-3.5	-3.2	-3.0
s_{21}	-0.35	-3.3	-3.5	-3.2	-3.0
s_{13}	-7.1	-3.2	-3.1	-3.4	-3.6
s_{31}	-7.1	-3.2	-3.1	-3.4	-3.6
s_{23}	-7.1	-3.2	-3.1	-3.4	-3.6
s_{32}	-7.1	-3.2	-3.1	-3.4	-3.6
s_{33}/s_{11}	5.1	0.97	0.86	1.03	1.16
s_{13}/s_{12}	20.3	0.97	0.89	1.06	1.20

Geometric mean average + biaxial stress state

Ferroelectric PMN-PT films

J. Ricote, DMF-Madrid

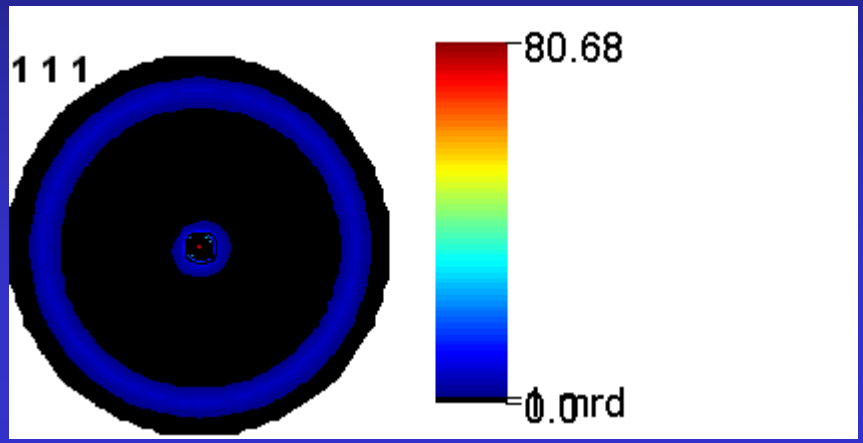

Pt

a = 3.91172(1) Å
T = 583(5) Å
t_{iso} = 960(1) Å
ε = 0.0032(1) rms
σ_{11}= 0.639(1) GPa
σ_{22}= 0.651(1) GPa
σ_{12}= -0.009(1) GPa

$Pb_{0.7}(Mg_{1/3}Nb_{2/3})O_3$-$Pb_{0.3}TiO_3$ /$Ti0_2$/Pt/Si-(100)

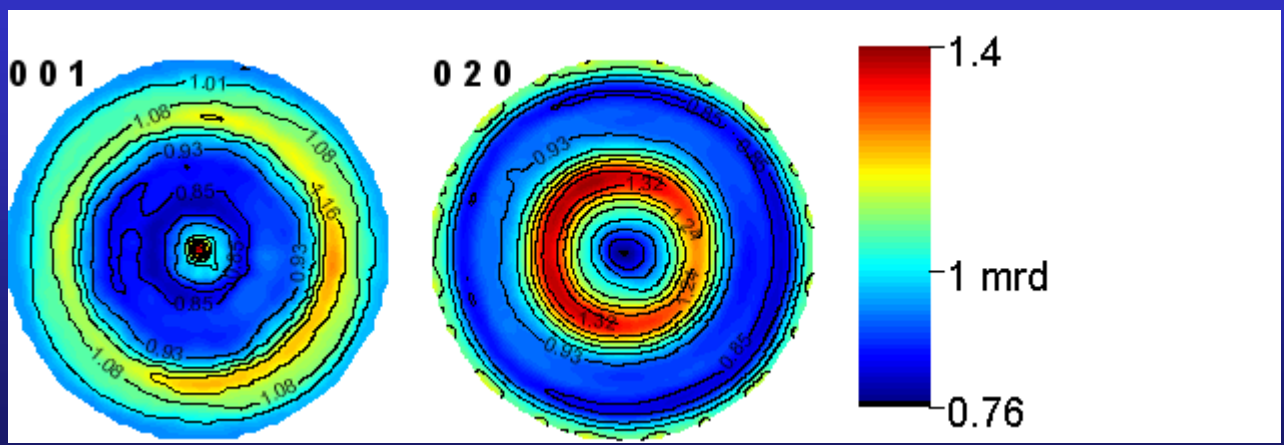

a = 5.67858(9) Å
b = 5.69038(9) Å
c = 3.99558(4) Å
β = 90.392(1) Å
T = 1322(9) Å
t_{iso} = 1338(2) Å
ε = 0.0067(1) rms

Si nanocrystalline thin films

M. Morales, Caen

Silicon thin films deposition by reactive magnetron sputtering:

- power density 2W/cm^2
- total pressure: $p_{total} = 10^{-1}$ Torr
- plasma mixture: H_2 / Ar, $pH_2 / p_{total} = 80$ %
- temperature: 200°C
- substrates: amorphous SiO_2 (a-SiO_2)
  (100)-Si single-crystals
- target-substrate distance (d)
  - a-SiO_2 substrates: d = 4, 6, 7, 8, 10, 12 cm
    films A, B, C, D, E, F
  - (100)-Si: d = 6, 12 cm
    films G, H

Aim: quantum confinement, photoluminescence properties

Typical refinement

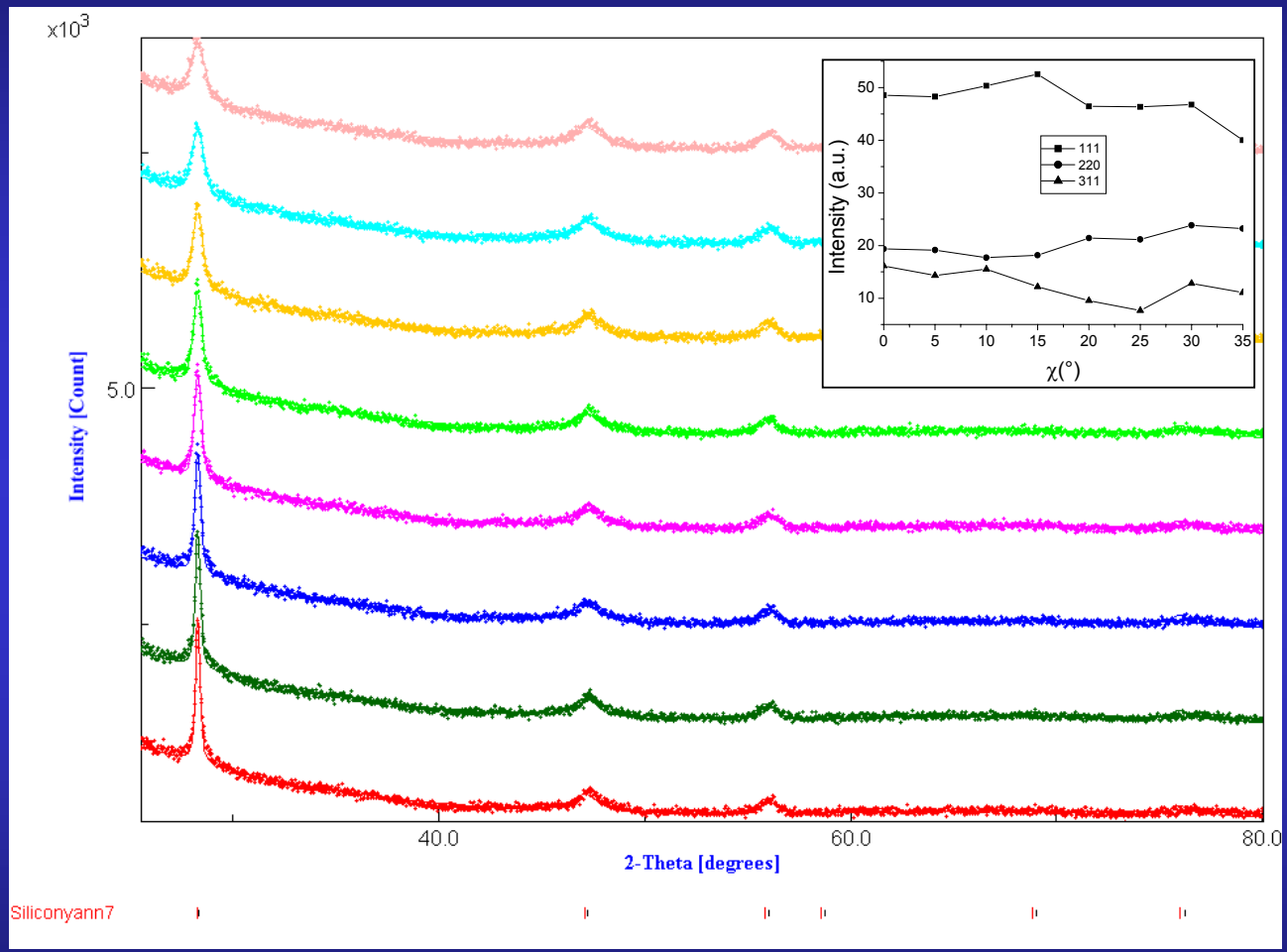

broad, anisotropic diffracted lines, textured samples

Refinement Results

Sample	d (cm)	a (Å)	RX thickness (nm)	Anisotropic sizes (Å)			Texture parameters			Reliability factors (%)			
				<111>	<220>	<311>	Maximum (m.r.d.)	minimum (m.r.d.)	Texture index F^2 (m.r.d^2)	RP_0	R_w	R_B	R_{exp}
A	4	5.4466 (3)	—	94	20	27	1.95	0.4	1.12	1.72	4.0	3.7	3.5
B	6	5.4439 (2)	711 (50)	101	20	22	1.39	0.79	1.01	0.71	4.9	4.3	4.2
C	7	5.4346 (4)	519 (60)	99	40	52	1.72	0.66	1.05	0.78	4.3	4.0	3.9
D	8	5.4461 (2)	1447 (66)	100	22	33	1.57	0.63	1.04	0.90	5.5	4.6	4.5
E	10	5.4462 (2)	1360 (80)	98	20	25	1.22	0.82	1.01	0.56	5.0	3.9	4.0
F	12	5.4452 (3)	1110 (57)	85	22	26	1.59	0.45	1.05	1.08	4.2	3.5	3.7
G	6	5.4387 (3)	1307 (50)	89	22	28	1.84	0.71	1.01	1.57	5.2	4.7	4.2
H	12	5.4434 (2)	1214 (18)	88	22	24	2.77	0.50	1.12	2.97	5.0	4.5	4.3

Mean anisotropic shape

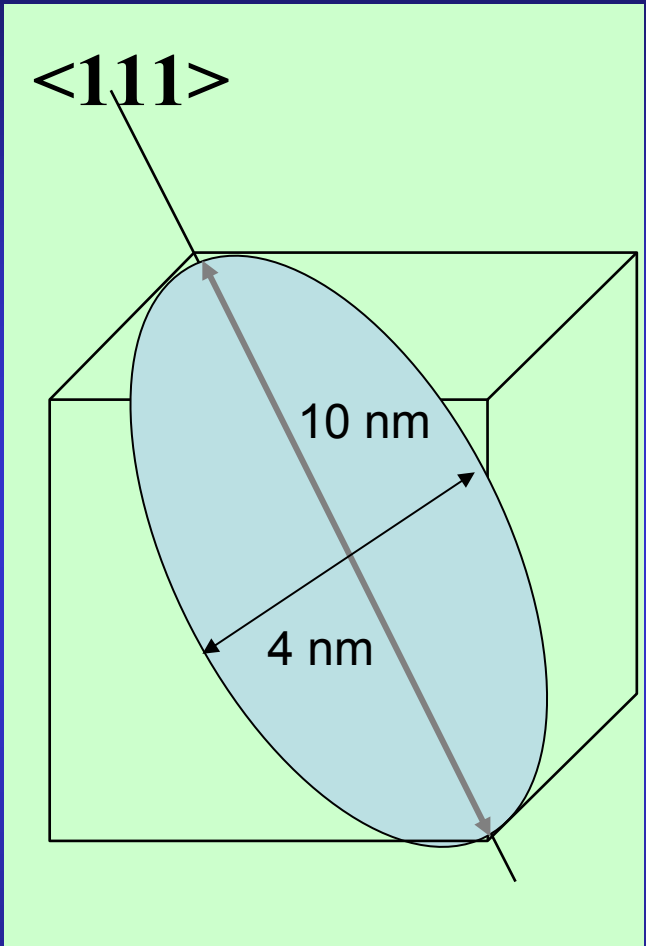

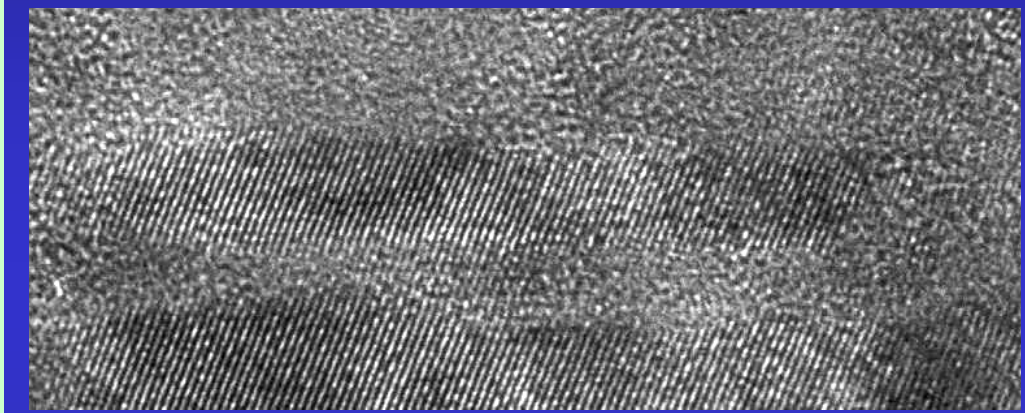

Schematic of the mean crystallite shape for Sample D represented in a cubic cell, as refined using the Popa approach and exhibiting a strong elongation along <111>, and TEM image

001 Inverse Pole Figures

a-SiO_2

(100)-Si

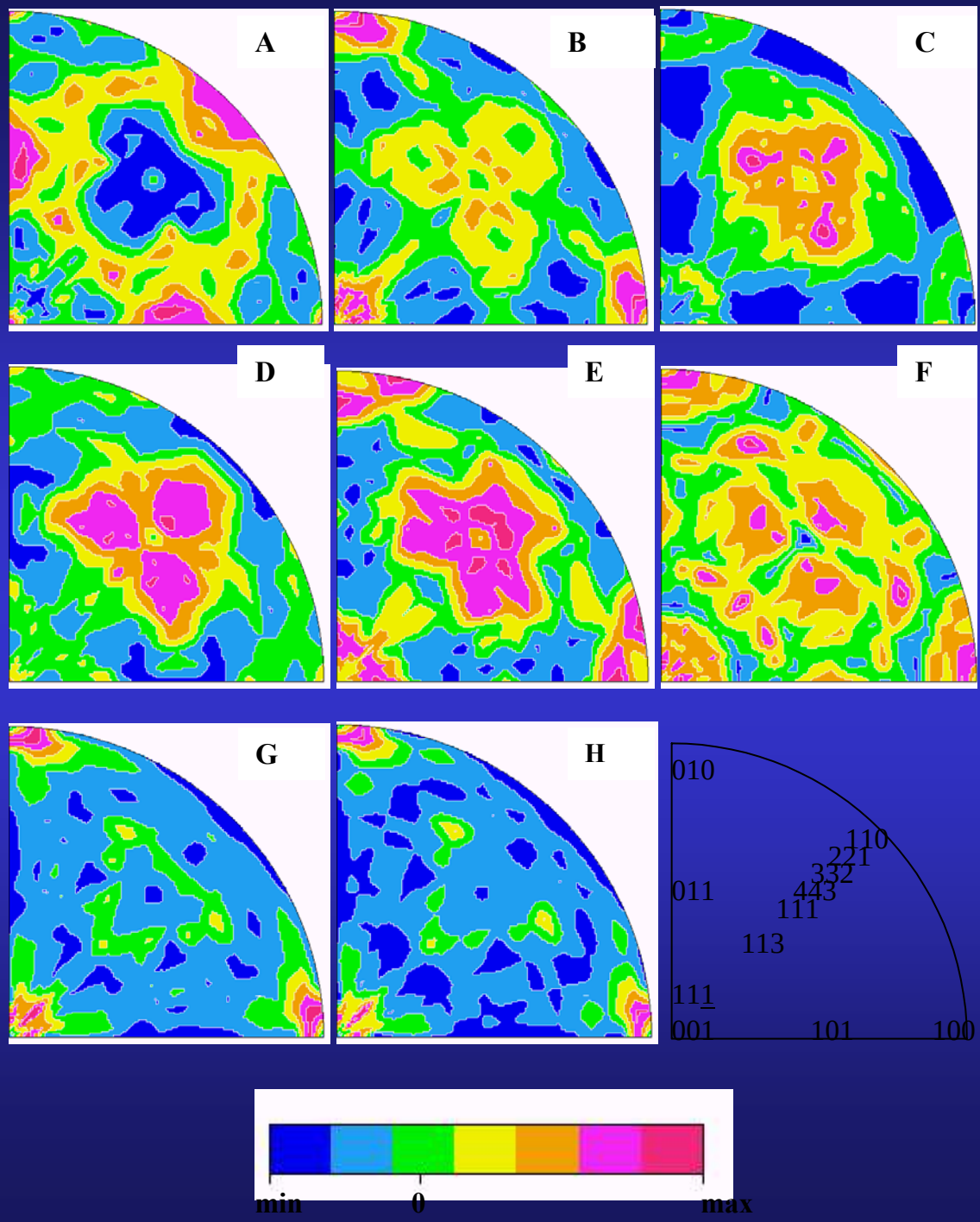

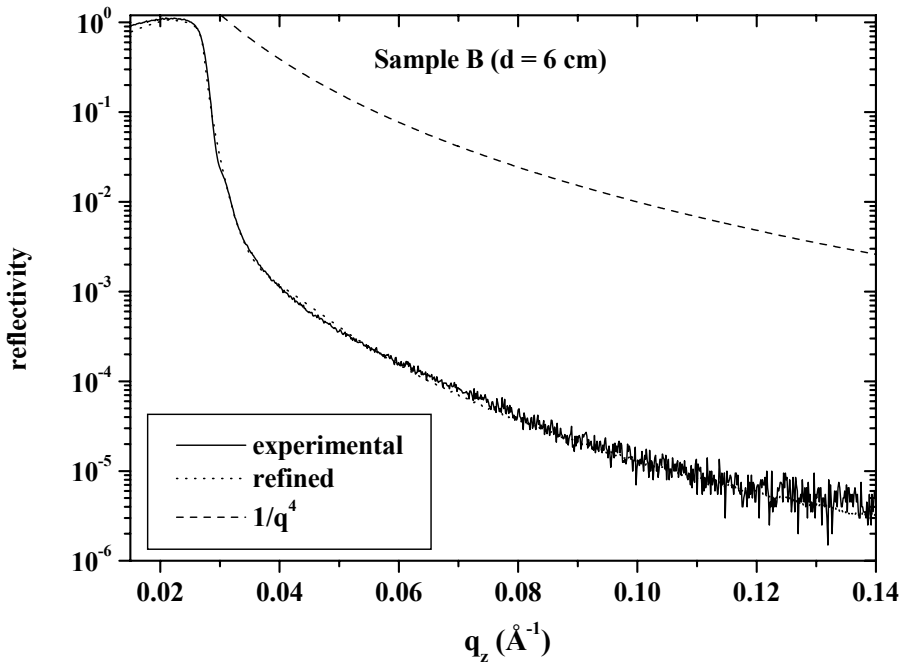

XRR:

Roughness governed

AFM:

homogeneous roughness

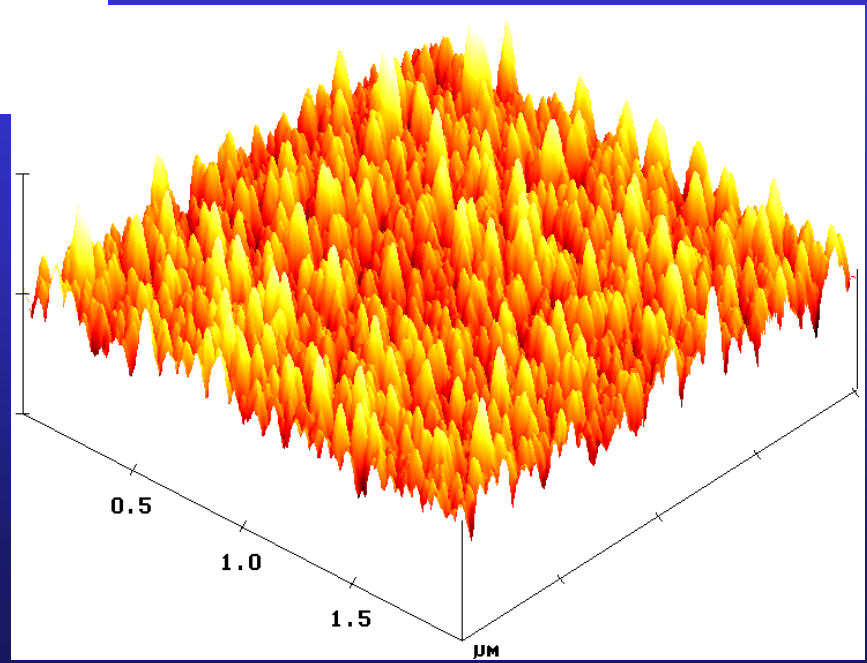

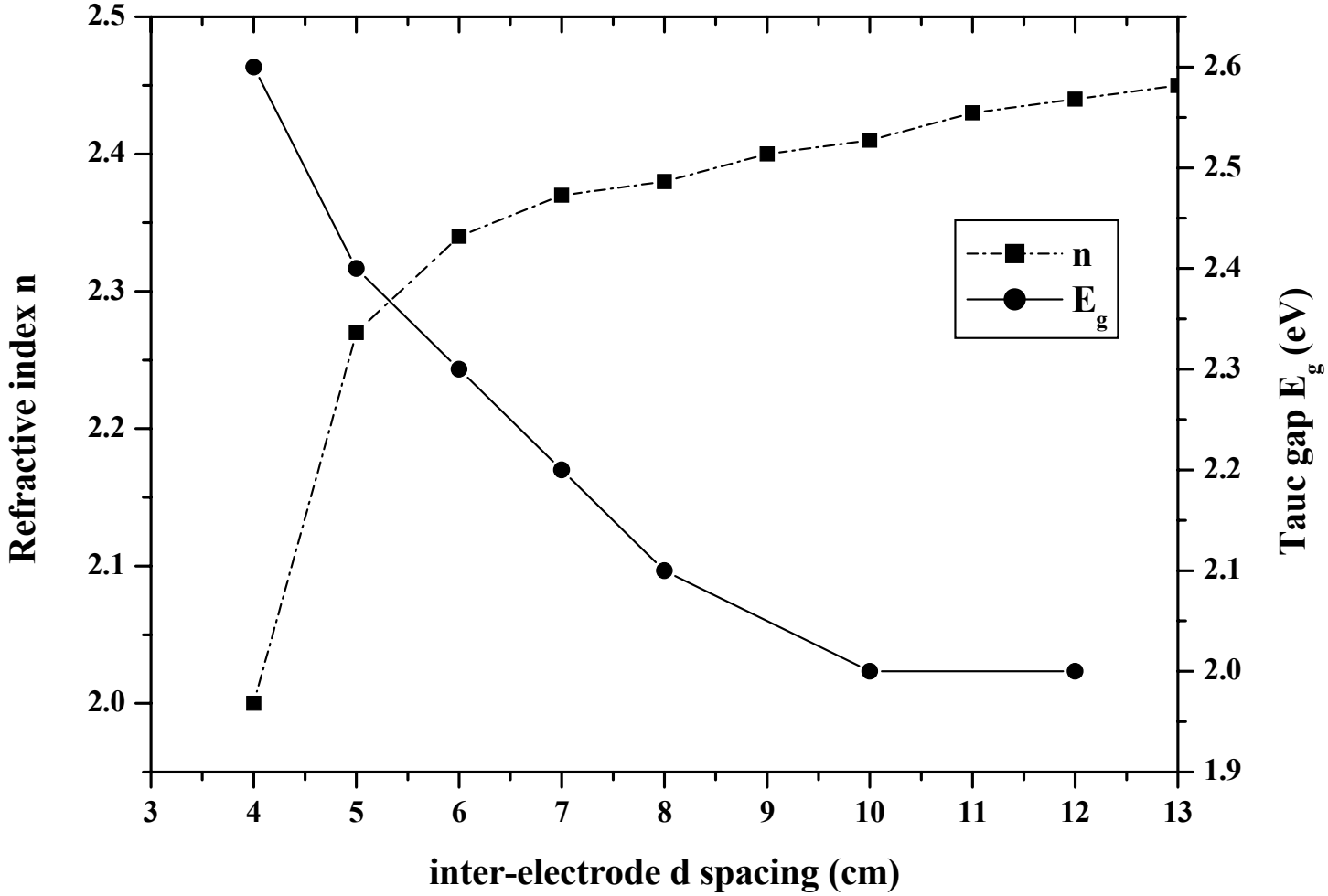
Refractive index n
Tauc gap E_g (eV)
inter-electrode d spacing (cm)
n
E_g
2.5
2.4
2.3
2.2
2.1
2.0
2.6
2.5
2.4
2.3
2.2
2.1
2.0
1.9
3
4
5
6
7
8
9
10
11
12
13

Irradiated FluorApatite (FAp) ceramics

S. Miro, PhD

Self-recrystallisation under irradiation, depending on SiO_4 / PO_4 ratio (FAp / Nd-Britholite) and on irradiating species

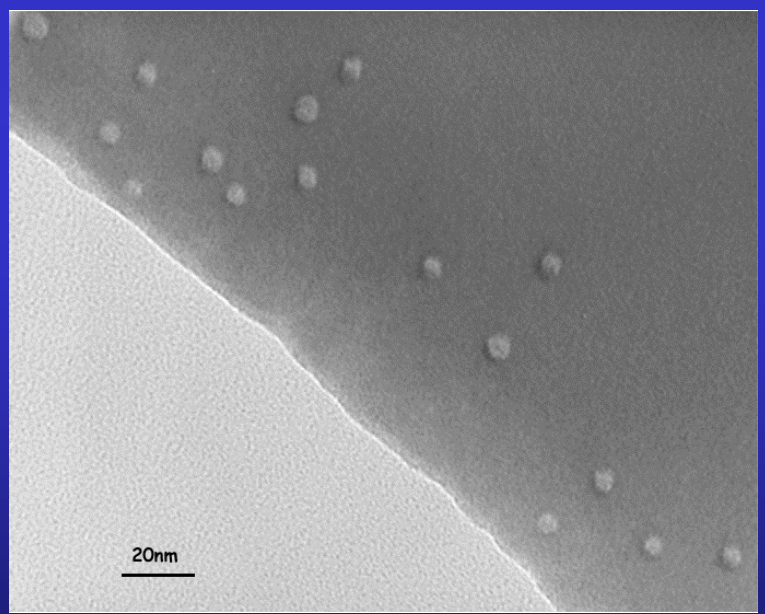

TEM of FAp irradiated with 70 MeV, 10^{12} Kr cm^{-2} ions

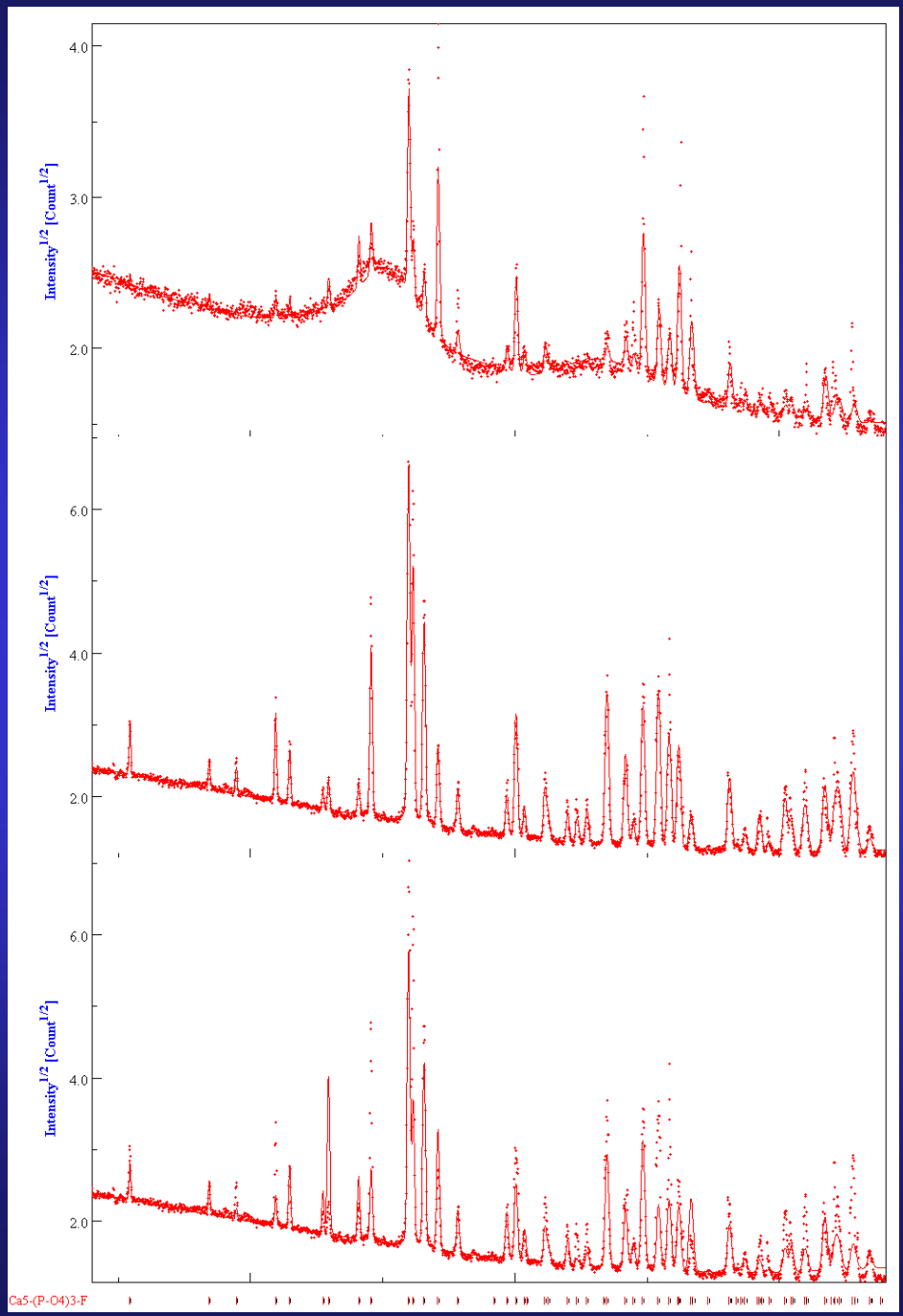

texture corrected,

10^{13} Kr cm^{-2}

Virgin, with texture correction

Virgin, no texture correction

Fluence (ions.cm^{-2})	Vc/V (%)	A (Å)	c (Å)	<t> (nm)	$\Delta a/a_0$ (%)	$\Delta c/c_0$ (%)	R_w (%)	R_B (%)
0	100	9.3365(3)	6,8560(5)	294(22)	-	-	14.6	9.1
Kr								
10^{11}	100	-	-	-	-	-		
10^{12}	100	-	-	-	-	-		
5.10^{12}	49(1)	9.3775(9)	6.8912(8)	294(20)	0.44	0.53	24	15
10^{13}	20(1)	9.4236(5)	6.9105(5)	291(20)	0.94	0.82	9.9	6
5.10^{13}	14(1)	9.3160(4)	6.8402(5)	294(22)	-0.21	-0.22	10.5	5.9
I								
10^{11}	-	-	-	-	-	-		
5.10^{11}	86(2)	9.3603(3)	6.8790(5)	90(10)	0.26	0.35	23.9	15.1
10^{12}	-	-	-	-	-	-		
3.10^{12}	47(2)	9.3645(3)	6.8840(5)	91(6)	0.30	0.42	13.3	9
5.10^{12}	29.2(5)	9.3765(5)	6.8881(6)	77(11)	0.44	0.48	10.4	7.3
10^{13}	13.2(2)	9.3719(4)	6.8857(6)	82(9)	0.38	0.45	6.7	4.9

Single impact model associated to crystal size reduction

Cell parameters and volume increase, then relax

Amorphisation / recrystallisation competition: single or double impact

Amorphous/crystalline volume fraction (damaged fraction Fd = Va / V) as determined by x-ray diffraction

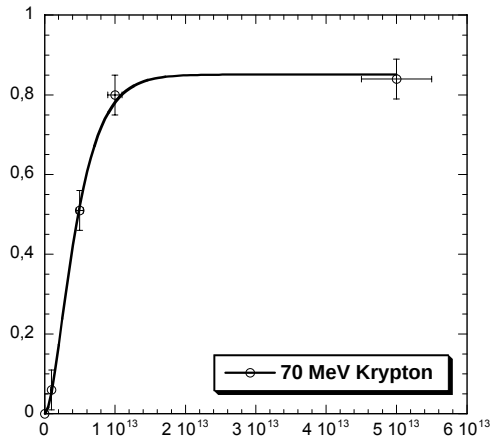

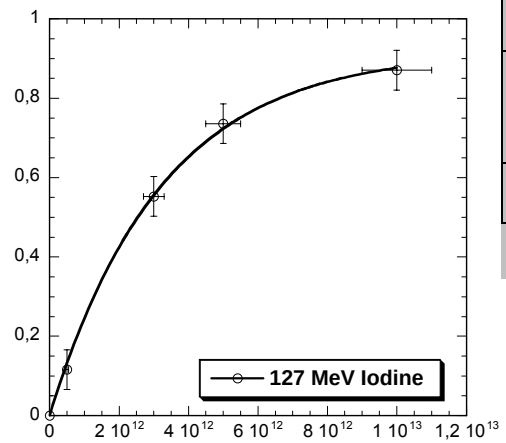

B

Fitting parameters	Krypton		Iodine
	Single impact Fd = B(1- exp(-Aϕt))	**Double impact** Fd = B(1 – (1+ Aϕt) exp(-Aϕt))	**Single impact** Fd = B(1- exp(-Aϕt))
A = πR² (cm²)	1.85 ± 0.15 10^{-13}	4.1 ± 0.15 10^{-13}	3.3 ± 0.15 10^{-13}
Radius R (nm)	2.4 ± 0.2	3.6	3.2
B (Max.damage rate)	0.87	0.85 ± 0.2	0.92 ± 0.2
χ2	0.013	0.0006	0.0004

$AlN/Pt/TiO_x/Al_2O_3/Ni\text{-}Co\text{-}Cr\text{-}Al$

E. Derniaux, PhD

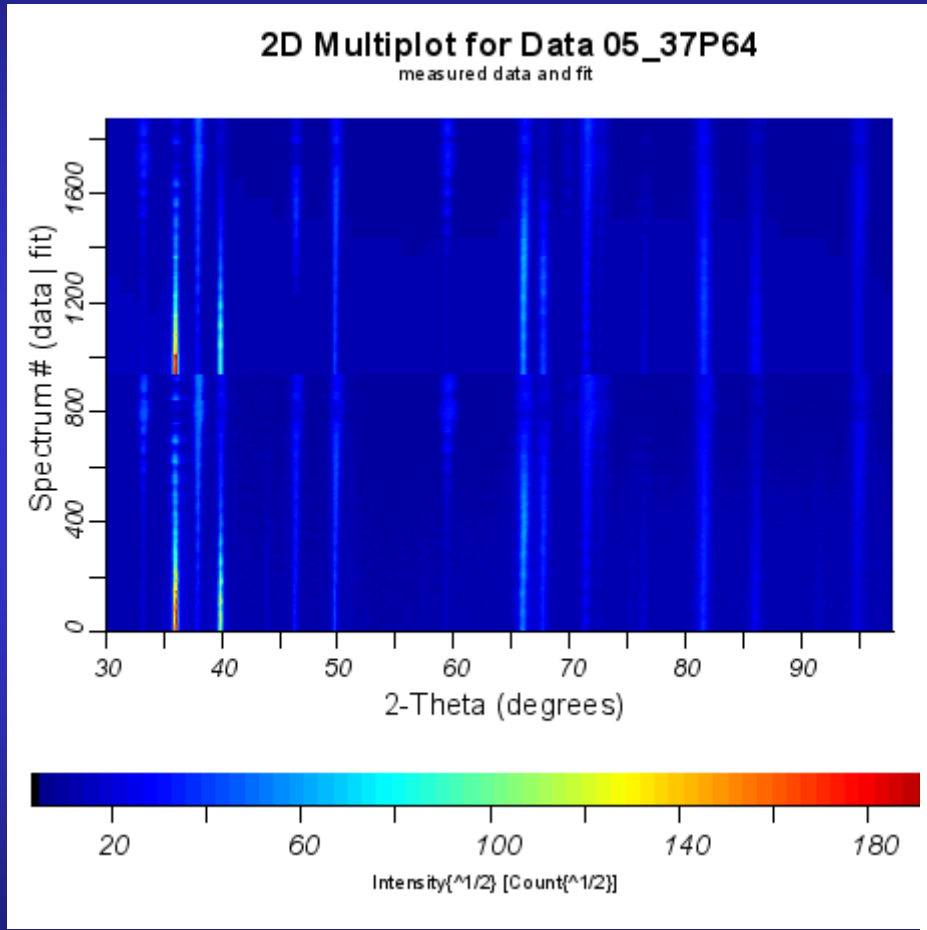

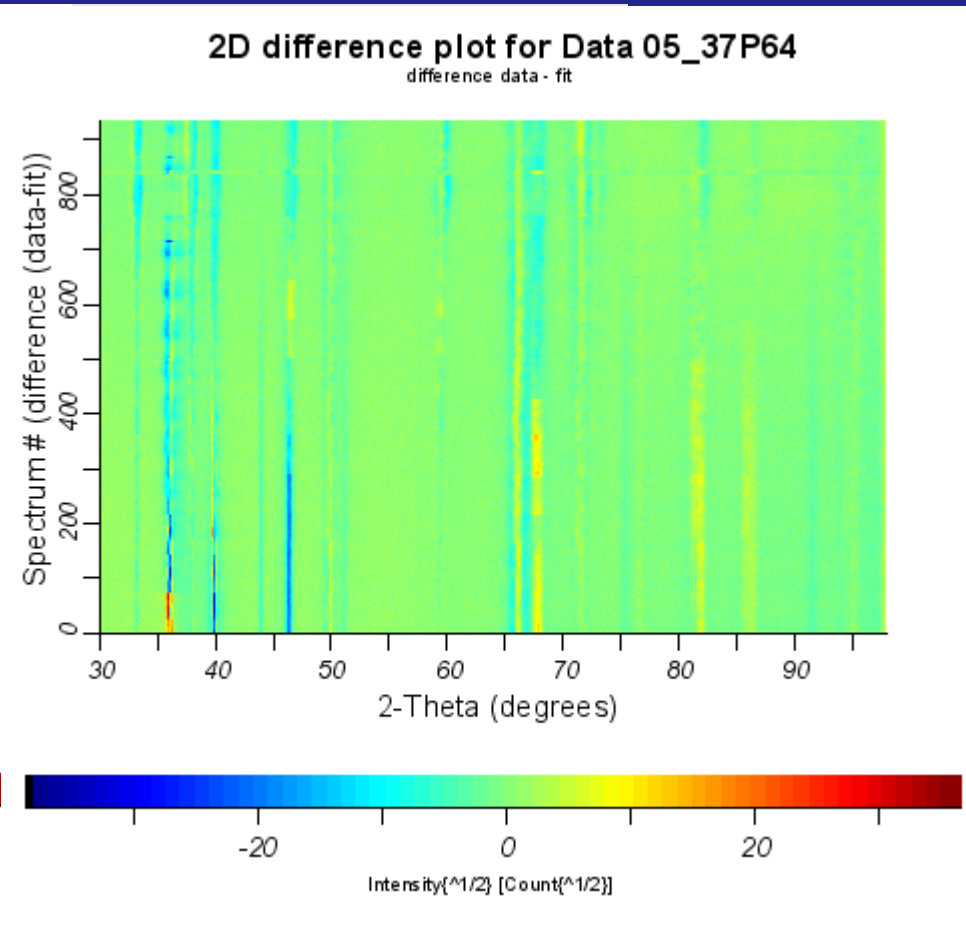

Rw (%) = 24.120445
Rexp (%) = 5.8517213

T(AlN) = 14270(3) nm
T(Pt) = 430(3) nm

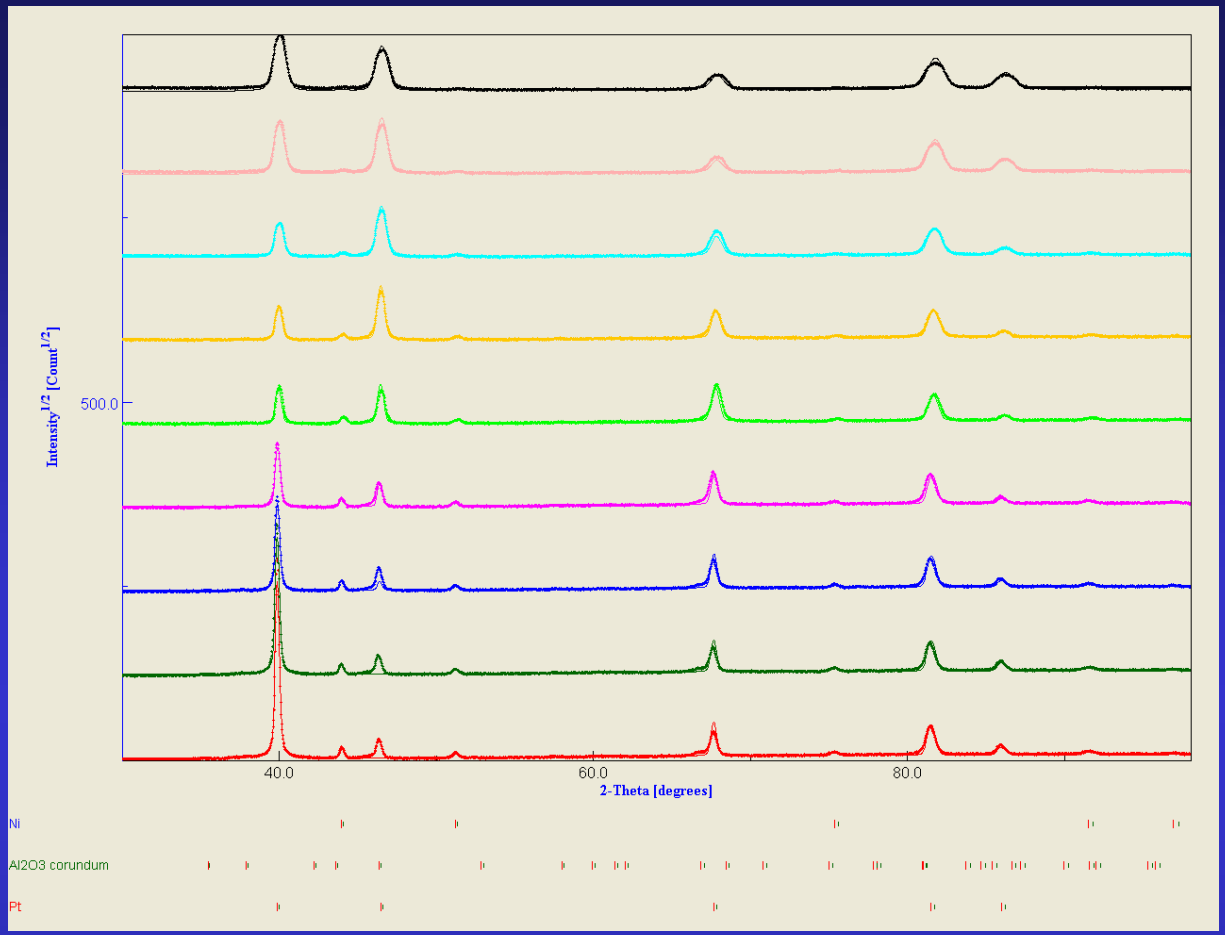

(χ,φ) randomly selected diagrams

Al_2O_3

a = 4.7562(6) Å
c = 12.875(3) Å
T= 7790(31) nm
<t> = 150(2) Å
<ε> = 0.008(3)

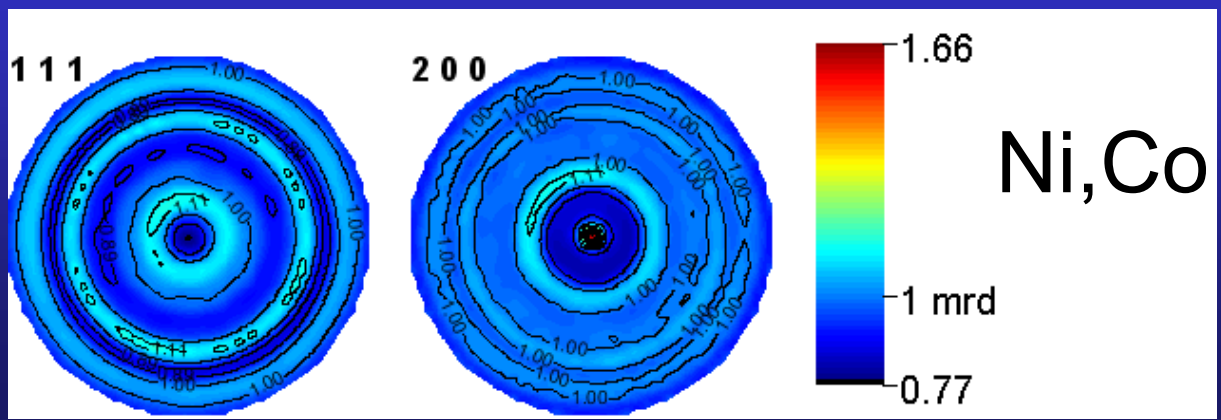

a = 3.569377(5) Å
<t> = 7600(1900) Å
<ε> = 0.00236(3)
σ_{11} = -328(8) MPa
σ_{22} = -411(9) MPa

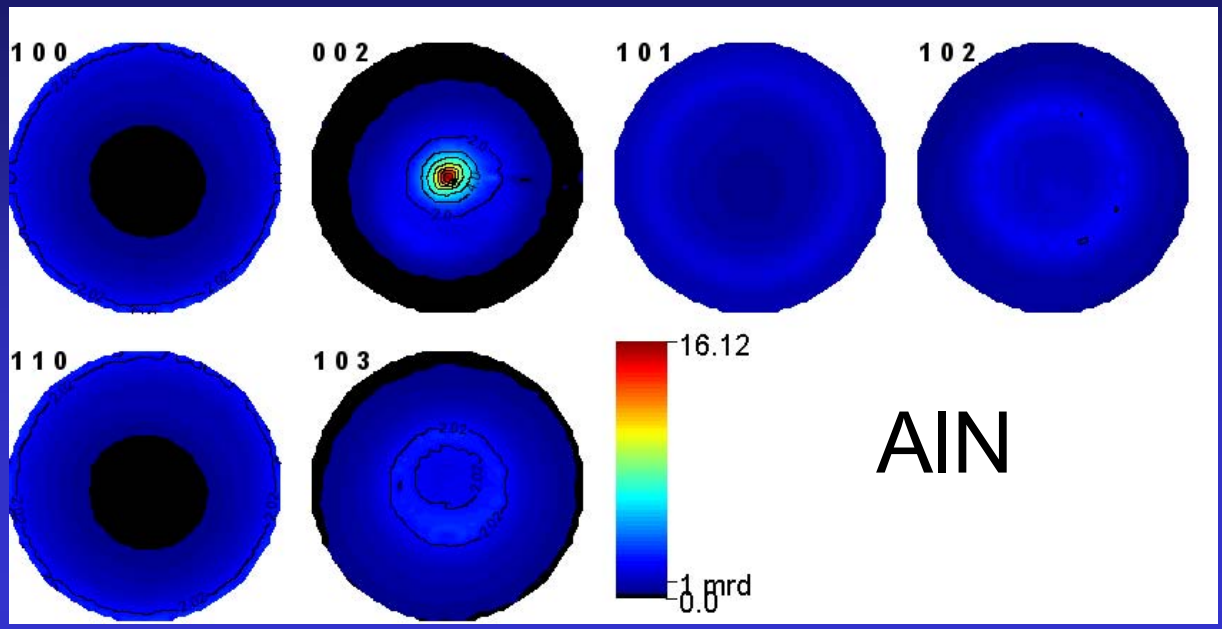

Rw (%) = 4.1

a = 3.11203(1) Å
c = 4.98252(1) Å
T = 14270(3) nm
<t> = 2404(8) Å
<ε> = 0.001853(2)
σ_{11} = -1019(2) MPa
σ_{22} = -845(2) MPa

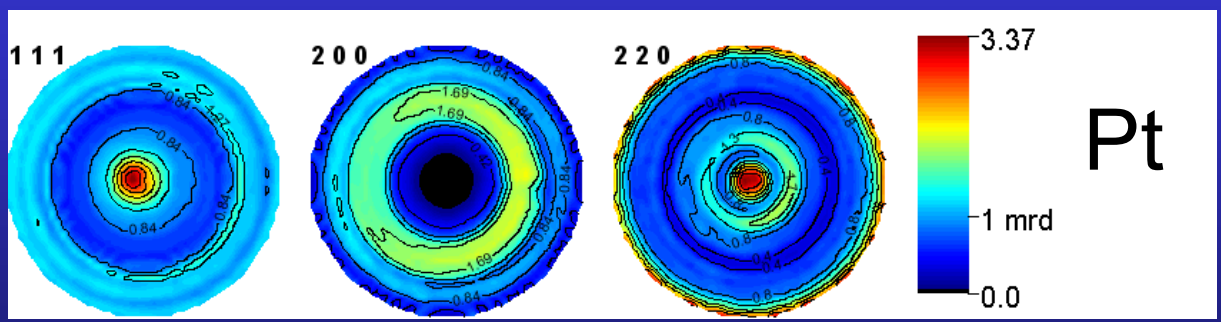

Rw (%) = 33.3

a = 3.91198(1) Å
T = 1204(3) nm
<t> = 2173(10) Å
<ε> = 0.002410(3)
σ_{11} = -196.5(8)
σ_{22} = -99.6(6)

Substrate bias vs stress-texture evolution

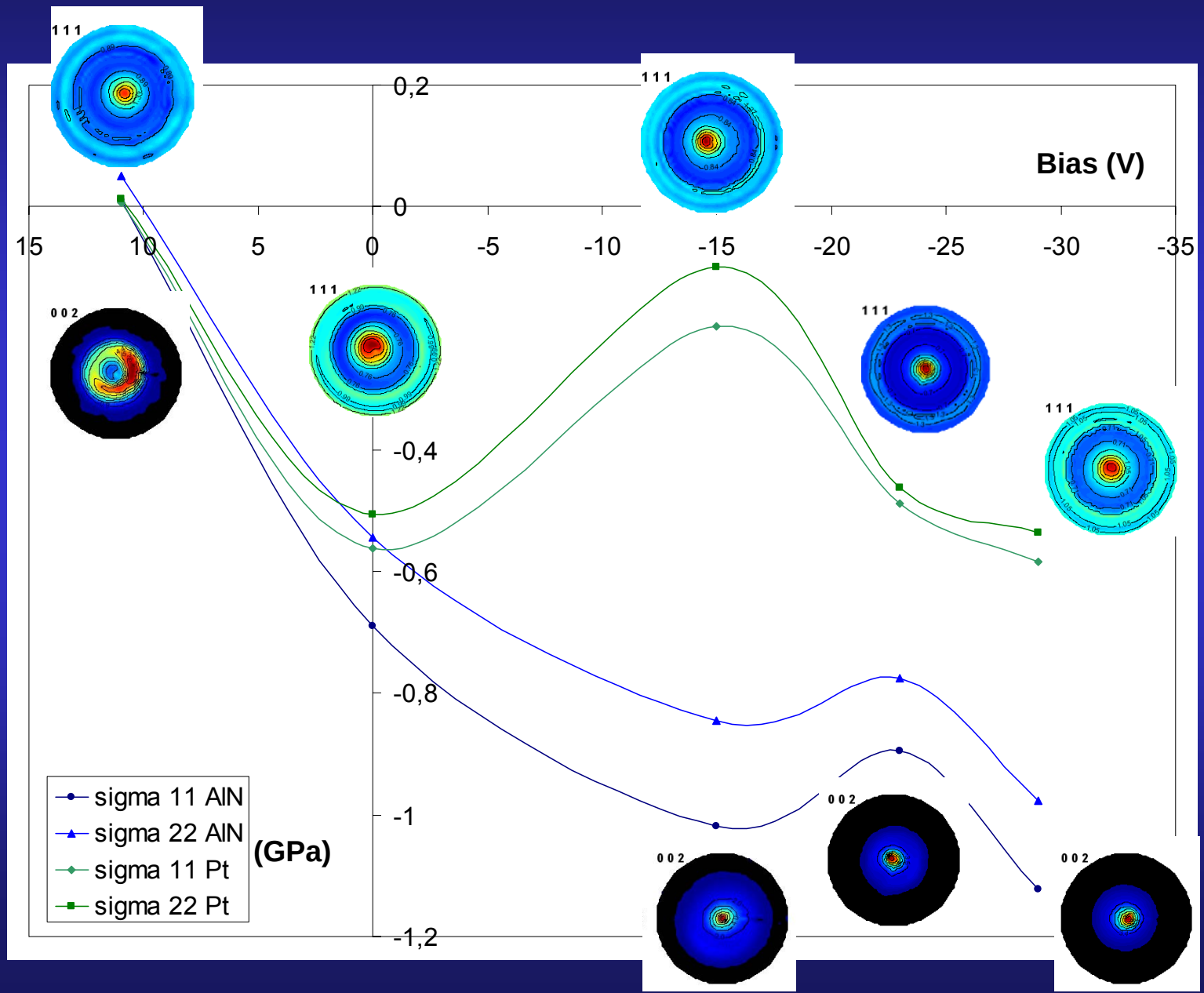

Conclusions

a) Texture affects phase ratio and structure determination

b) Microstructure (crystallite size) affects texture (go to a)

c) Stresses shift peaks then affects structure and texture determination

d) Combined analysis may be a solution, unless you can destroy your sample or are not interested in macroscopic anisotropy ...

e) If you think you can destroy it, perhaps think twice

f) more information is always needed: local probes ...

g) www.ecole.ensicaen.fr/~chateign/texture/combined.pdf